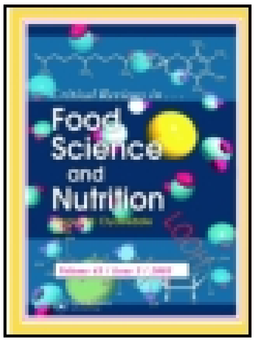

Critical Reviews in Food Science and Nutrition

ISSN: (Print) (Online) Journal homepage: https://www.tandfonline.com/loi/bfsn20

Trends in functional food development with three-dimensional (3D) food printing technology: prospects for value-added traditionally processed food products

Yusuf Olamide Kewuyemi, Hema Kesa & Oluwafemi Ayodeji Adebo

CRITICAL REVIEWS IN FOOD SCIENCE AND NUTRITION
https://doi.org/10.1080/10408398.2021.1920569

Taylor & Francis
Taylor & Francis Group

REVIEW

OPEN ACCESS
Check for updates

Trends in functional food development with three-dimensional (3D) food printing technology: prospects for value-added traditionally processed food products

Yusuf Olamide Kewuyemi[a], Hema Kesa[a], and Oluwafemi Ayodeji Adebo[b]

[a]School of Tourism and Hospitality, College of Business and Economics, University of Johannesburg, Gauteng, South Africa; [b]Department of Biotechnology and Food Technology, Faculty of Science, University of Johannesburg, Gauteng, South Africa

ABSTRACT
One of the recent, innovative, and digital food revolutions gradually gaining acceptance is three-dimensional food printing (3DFP), an additive technique used to develop products, with the possibility of obtaining foods with complex geometries. Recent interest in this technology has opened the possibilities of complementing existing processes with 3DFP for better value addition. Fermentation and malting are age-long traditional food processes known to improve food value, functionality, and beneficial health constituents. Several studies have demonstrated the applicability of 3D printing to manufacture varieties of food constructs, especially cereal-based, from root and tubers, fruit and vegetables as well as milk and milk products, with potential for much more value-added products. This review discusses the extrusion-based 3D printing of foods and the major factors affecting the process development of successful edible 3D structures. Though some novel food products have emanated from 3DFP, considering the beneficial effects of traditional food processes, particularly fermentation and malting in food, concerted efforts should also be directed toward developing 3D products using substrates from these conventional techniques. Such experimental findings will significantly promote the availability of minimally processed, affordable, and convenient meals customized in complex geometric structures with enhanced functional and nutritional values.

KEYWORDS
3D food printing; fermentation; healthy food structures; malting; novel food ink; traditional foods

1. Introduction

3D printing, popularly known as additive manufacturing, is an automated manufacturing process that works either by depositing layers of raw materials or binding raw materials to create physical 3D structures (Lipson and Kurman 2013). The printing technology has received keen attention from the industry, public, and academia for its many advantages (García-Segovia et al. 2020; Le-Bail, Maniglia, and Le-Bail 2020; Piyush, Kumar, and Kumar 2020). According to Alexander (2020), on a global market scale, 3D printing products and services are anticipated to have a yearly growth rate of about 26% and envisaged to worth 40 billion US dollars by 2024. The potential advantages of 3D printing technology are being maximized within the food sector include: customized food design, digitalized and personalized nutrition, efficient use of raw material, and expansion of food material source (Anukiruthika, Moses, and Anandharamakrishnan 2020; García-Segovia et al. 2020), with potential for much more. Printed foods also help improve the overall appeal of meals, which could reduce children and other age groups' reluctance to eat specific food ingredients (Hamilton, Alici, and In Het Panhuis 2018; Derossi, Husain, et al. 2020). Also, such foods could satisfy the demand of narrow consumer groups like vegetarians and the elderly with chewing or swallowing and digesting difficulties (Kira 2015; Hua, Na, and Dong 2018). These will further create a potential market and demand for food printing. Sun et al. (2018) highlighted the current drawbacks of food printing: limited use of ingredients and the public's general preference for traditionally made foods. While the need to meet changing lifestyles and demand for minimally processed foods and convenient foods continues to dictate innovations in the food industry, there is still the demand for traditionally processed foods.

Fermentation and malting are traditional, and age-long food processing/culinary practices used to transform food for consumption. The former is a complex bioprocess that is aided by natural flora or inoculation of suitable microbial strains to evoke biotransformation of food materials' inherent constituents. Resultant products are often accompanied by desired modification in nutrients and bioavailability, and organoleptic properties (Adebo 2020; Kewuyemi, Kesa, et al. 2020, Tamang et al. 2020). On the other hand, the latter is stimulated by the partial hydration of food grain and

CONTACT Hema Kesa hemak@uj.ac.za; oadebo@uj.ac.za School of Tourism and Hospitality, College of Business and Economics, University of Johannesburg, P.O. Box 524, Bunting Road Campus, Gauteng, South Africa.

intermittent moistening under controlled conditions to influence the substrate composition positively through the dynamic actions of hydrolytic enzymes. The presence of some health prompting bioactive components (polyphenols, bioactive peptides, phytosterols, soluble fibers, and other phytonutrients) have been reported in fermented and malted grain products (Adebiyi et al. 2017; Adebo and Medina-Meza 2020; Kewuyemi, Njobeh, et al. 2020). Furthermore, ingestion of such fermented or malted products has been reported to potentially enhance the host immune system's health conditions and reduce the risk of metabolic-related syndromes associated with chronic diseases (Singh and Sharma 2017; Gong et al. 2018; Bationo et al. 2020).

Malted and fermented foods (MFFs) comprise part of the identity of many ethnic groups, with an estimate suggesting that fermented foods and related products provide about a third of the world food supplies (Xiang et al. 2019). Despite their huge contribution to food security, these foods are still being produced mainly at small-scale levels, thus the need to upscale for industrial production (Tamang et al. 2020). Hence, the development and delivery of value-added MFF products through the integration of 3DFP will be a fusion of the dying old (traditional food processes) and emerging new (3DFP), which holds enormous potential for innovative 3D food structures. Such nutritionally rich and functionally potent edibles exhibiting high geometric complexity would promote their broader acceptability.

This review provides an overview of the 3DFP process. It discusses the major factors, including the suitability of edible inks for 3D printing purposes, printing parameters, and complementary post-processing treatments affecting the process development of successful edible 3D structures. The summary of available literature on extrusion-based 3D printed foods was used as a context to presents the potential applicability of 3D printing for fermented and malted foods. Advantages and challenges stemming from those studies were highlighted for possible scale-up. Future trends and future direction on developing functional 3D printed foods were emphasized to enhance the global acceptance of an innovative and emerging continuous food processing technology. This review is expected to drive considerable interest in promoting traditionally processed foods as a natural alternative and affordable edible meals presented in novel forms within the current trends of consumers' healthier diets.

2. Overview of 3DFP process

Various techniques of 3DFP technologies have been implemented in the food industry, including binder jetting, inkjet printing, extrusion-based printing, and selective laser sintering (Liu and Zhang 2019). Their printing-driven mechanism distinguishes these technologies. The extrusion-based 3DFP technique, also referred to as fused deposition modeling (FDM), is best suited for food applications due to its design flexibility and support for printing an extensive range of food materials such as confectionery, dough, gel, and puree products, among others.

Simple preparation for more innovative 3D printed edible constructs may comprise milling grain-like material, followed by hydration, mixing to attain dough/paste-like consistency, or the material or mixture subjected to bio-modification for more compositional value. Other food substrates preparation modes may encompass screening of coarse or oversized particulates, stabilizing, homogenizing, and de-aerating to enhance an even and continuous filament printing (Nijdam, Agarwal, et al. 2021). Such printed products may be presented as complex food geometries with consistent processing features to offer new dining experiences (Mantihal, Prakash, and Bhandari 2019a). Similarly to the conventional food extrusion process (Wójtowicz and Mościcki 2014; Sobowale et al. 2018), 3DFP can either be a hot extrusion (HE) process in which case; resultant products require no further post-processing or cold extrusion (CE) in which 3D printed foods (3DPF) usually requires a cooking step such as baking, frying, drying, or steaming (Anukiruthika, Moses, and Anandharamakrishnan 2019; Feng et al. 2020; Liu, Bhandari, et al. 2020). The latter is applied, especially when printing is done at extrusion temperatures $\leq 50\,^{\circ}C$, the printing temperature range at which printing behavior or cooking effect (such as dehydration) on some foods may be less significantly affected (Liu, Tang, Duan, Qin, Zhao, et al. 2020; Paolillo et al. 2021).

Irrespective of the approach, the digital nature of 3DFP requires a virtual 3D model, which is further programmed with inputs via an available user interface, either online or offline computer-aided design (CAD) application software, to execute the planned printing route (Figure 1). In clear terms, the process involves conceptualization and subsequent generation of a CAD 3D model embedded in standard tessellation language file format →.stl file, predefining the path printing conditions (such as extruding temperature, nozzle size, printing speed, layer height, percentage substrate flow, etc.) using a slicing software that generates commands in g-code format →.gcode file, the readable standard printing language for 3D food printers. The prepared food mix in dough/paste-like consistency or puree, often termed as "food ink," is fed into the extrusion mechanism container. The 3D printer is then initiated after loading the .gcode file, and a layer-by-layer deposition of the food ink commences to form an edible 3D structure. The obtained product could be consumed (if pre-cooked before printing or hot extruded), or the formed 3D printed structure is kept at freezing or refrigeration temperature. It is, therefore, ready for another phase of post-processing such as frying, steaming, baking, etc. (if cold extruded).

Open-source platforms and software applications for the creation of 3D food designs include Tinkercad (Autodesk, Inc., San Rafael, CA), Thingiverse (MakerBot Industries, Brooklyn, CA), AutoCAD (Autodesk, Inc.), Meshmixer (Autodesk, Inc.), etc. Digital models may also be created by 3D scanning solid objects and reversing them into virtual designs (Guo, Zhang, and Bhandari 2019a). For the slicing process, commonly used software are Repetier-Host (Hot-World GmbH & Co. KG, Willich, Germany), Slic3r (Microsoft), Cura (Ultimaker B.V., The Netherlands), and Rhinoceros/Rhino 3D (Robert McNeel & Associates) (Table 1). The slicing software's choice depends on the best compatibility with the 3D printer available for use or its recommended slicing package by the manufacturer. The

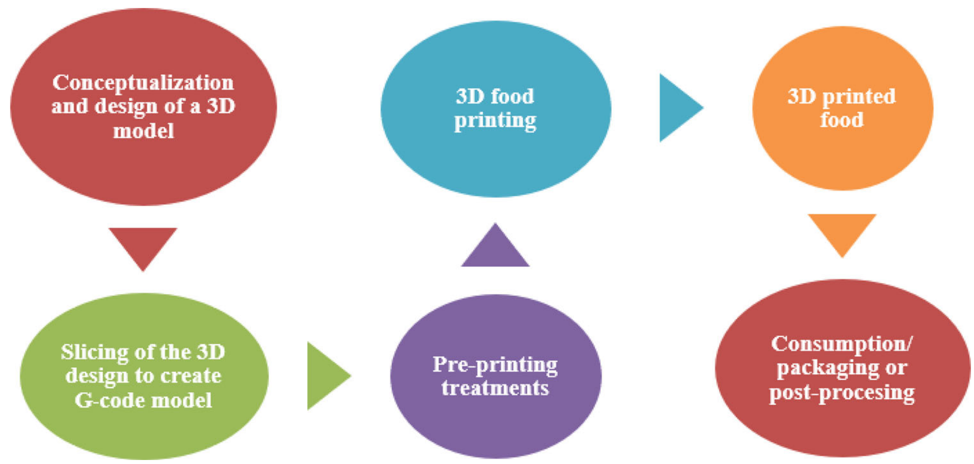

Figure 1. An overview of the 3D food printing process.

major 3D food printers maybe in the form of Cartesian, Delta, Polar, or Scara configurations (Derossi et al. 2019). These configurations describe the printhead movement or print stage in a chamber comprising X, Y, and Z axes (Figure 2). These configurations' scope presents varying suitability and limitations in the food printing application, with the Cartesian and Delta designs being the most used configurations for 3DFP.

Schematically, the food extrusion printer consists of four major body parts; the printhead [feed hopper, feed barrel/ syringe/cartridge, extruding head(s)], digital control interface, print stage, and moveable case. The printing process is governed by either screw-based or syringe-based extrusion mechanisms (Figure 3). These compartments serve as a temporary container during extrusion, attached with a force driving device (usually pneumatic pump or stepper motor) acting linearly. Subsequently, food material deposit can be obtained via the nozzle tip on the print stage. Various food ink types, either in semi-liquid/solid or low/high viscous forms, are adaptable with the printing mechanisms (Table 1). Several other factors, including food materials' properties, printing parameters, and post 3D structure processing, are equally considered to achieve successful edible 3D constructs, which are defined by its printing quality; precision, accuracy, and shape stability (Yang, Zhang, Prakash, et al. 2018; Yang, Zhang, Fang, et al. 2019; Phuhongsung, Zhang, and Devahastin 2020). These factors affecting 3DFP are discussed in the next section of this review.

3. Factors affecting printability of 3D food products

3.1. Printability of food material

In 3DFP, food materials prepared for printing are commonly referred to as "food ink." Lee et al. (2019) defined a food ink system's printability as the properties that denote its fluidity for smooth extrusion and mechanical strength required to maintain its mass and prevent deformation during a 3D printing operation. Printability of a food ink could also mean the ease and uniformity of extrusion from a thin nozzle tip with accurate and precise printing dimension and its ability to adhere to printing layers evenly, retain smooth and compact structure during printing and post-deposition. The term may also be associated with the extrudability, flowability, and post-processing stability of a well-developed structure (Pulatsu and Lin 2021). These printability characteristics also affect the printed object's overall resolution, which may define its fidelity of printing, i.e., the ability to create an excellent replica of a CAD model (Kim, Bae, and Park 2018; Paolillo et al. 2021). Foods of a gelly nature or containing significant amounts of starch/hydrocolloids are generally printable, relatively to the gel's quality indicated by elasticity, viscosity, and water molecule mobility (An et al. 2019). According to Dankar, Haddarah, et al. (2018), such materials should ideally be stable enough to hold their shape after deposition.

Notwithstanding, the practical realization of superior printing performance and characteristics of an edible material largely depends on its composition and morphological characteristics (Pulatsu and Lin 2021). These are key determining factors that are best described by flow behavior and rheological data for printing applications. Materials exhibiting non-printable characteristics may be modified in several ways, including the addition of additives, the addition of enzymes, adjusting the solid/liquid component concentration of the material, minor processing to adjust physical characteristics, use of pretreatment techniques, and storage conditions before printing experiment (Table 1). The degrees of modifications thereof for proper printability of some inks are further discussed in the next sub-sections.

3.1.1. Choice of printable substrate

Printability of materials might have indeed contributed to the lesser number of available 3DPFs in the market. Particularly fermented and malted grains, which could serve as printing substrates, may not generally be printable by nature. According to Gholamipour-Shirazi, Norton, and Mills (2019), 3D printing ink must possess both liquid-like characteristics (to be flowable during extrusion shear effect) and solid-like characteristics (to be printable into a self-supporting structure after deposition). To thus facilitate potential inks' printability: appropriate preprinting treatments are done. As summarized in Table 1, natural or other food-

Table 1. Summary of available studies on 3D printed food items based on extrusion technique.

Material composition	Optimized/printable ink formulation	3D model source/ slicing software	3D Printer used and structural configuration	Printing temperature and classification of 3DFP	Extrusion mechanism and optimal printing parameters	Post-processing operation	Product	Reference
Cereal/pseudo cereal-based								
Dough (low gluten flour, butter, eggs, icing sugar, and water)	[(6.0 g butter, 10.4 g egg, 48.0 g flour, 6.6 g icing sugar, and 29 g water)/100 g]	NS	PORIMY Co. Ltd., Wuxi, China	24.8 °C CE	Screw type Nozzle diameter (2.0 mm), print speed (25 mm/s), and extrusion speed (118.689 mm^3/s)	NA	Printed dough	Yang, Zhang, Prakash, et al. (2018)
Dough (low gluten flour, butter, eggs, icing sugar, and water)	[(6.0 g butter, 10.4 g egg, 48.0 g flour, 6.6 g icing sugar, and 29 g water)/100 g]	Repetier	PORIMY Co. Ltd, Kunshan, China	24.8 °C CE	Filament diameter (2.30 mm), nozzle diameter (2.0 mm), nozzle movement speed (25 mm/s), and nozzle height (2.40 mm)	Fast cooling (at −65 °C for > 10 min) and baking (190 °C for 10 min)	Printed dough	Yang, Zhang, Fang, et al. (2019)
Paste [brown rice flour, guar gum (GG), xanthan gum (XG), and water]	Steamed brown rice flour (100 g), water (300 g), XG-GG, 3:2 wt/wt (1% wt/wt)	Repetier-Host	3D food printer (ShiYin Technology Co. Ltd., Hangzhou, China)	NS	Syringe type Print speed (20 mm/s), extrusion level (100%), nozzle size (0.84 mm), infill density (15, 45, and 75%), and perimeter (7)	NA	Printed object	Huang, Zhang, and Bhandari (2019)
Doughs (water, sunset yellow, indica, japonica, and waxy rice)	Indica rice: water (100:85), japonica rice: water (100:95), and sunset yellow (0.04%)	NS	Delta configuration. Chengdu Xinshunyun Biotechnology Co., Ltd., Chengdu, China	25 °C CE	Syringe driven by air pressure system Travel speed (20 mm/s), layer height (0.76 mm), shell thickness (1.52 mm) initial layer thickness (0.3 mm), infill density (100%), nozzle size (0.76 mm), and nozzle height (2.0 mm)	Steaming (at 100 °C for 30 min)	Printed rice-based foods	Liu, Tang, Duan, Qin, Zhao, et al. (2020)
Paste (sodium alginate, water, sunset yellow, indica, japonica, and waxy rice)	Japonica rice (100%), indica rice (100%), water (90% vol/wt), sodium alginate (0.5%) and sunset yellow (0.04%)	AutoCad Cura 15.0	Chengdu xinshunyun biotechnology Co., Ltd., Chengdu, China	25 °C CE	Syringe type Infill density (100%), layer height (0.76 mm), nozzle size (0.76 mm), nozzle height (2.0 mm), and travel speed (20 mm/s)	Steaming (at 100 °C for 30 min)	Printed rice products	Liu, Tang, Duan, Qin, Zhao, et al. (2020)
Dough (wheat flour and water)	Wheat flour (100 g) and water (54 g)	Tinkercad CURA 15.04.2	Delta 2040, Wasp project, Italy, and Clay extruder kit 2.00, Wasproject, Italy	Room temperature CE	Syringe type Infill density (15%), layer height (0.4 mm), nozzle size (0.6 mm), print speed (30 mm/s), and travel speed (50 mm/s)	Baking (at 200 °C for 15 min)	Printed Snacks	Severini, Derossi, and Azzollini (2016)
Dough [wheat flour (WF), butter, potato granules, sugar, and water]	High gluten WF (72 g), low gluten WF (108 g), butter (100 g), sugar (70 g), potato granules (20 g) and water (75 g)	NR	Food printer, XYZ Printing, Suzhou, China	35 °C CE	Syringe driven by stepper motor Nozzle diameter (2.0 mm) and flow rate (2.88 × 10^{-7} m^3/s)	NA	Printed dough	Liu, Chen, et al. (2020)
Cookie dough (wheat flour, powdered sugar, butter fat,	[Wheat flour (39.5 g) butter fat (25 g), milk (13 g),	NS	3D food printer (YL-CUBE, YOLILO, Korea)	CE	Syringe type Nozzle size (1.0 mm), nozzle movement speed	Baking (at 170 °C for 15 min)	Printed cookie dough	Kim et al. (2019)

milk, xanthan gum, and methylcellulose)	powdered sugar (22 g), and xanthan gum (0.5 g)]/100 g				(20 mm/s), first layer height (0.9 mm), and nozzle height (0.95 mm)			
Dough (wheat flour, dry mango powder, water, and olive oil)	Flour (57.5 g), water (30 g), mango powder (2.5 g), and olive oil (3 g)	Customized computer-based JAVA program	3D printing system (Lv Xin Co. Ltd., Chengdu, China)	Room temperature, CE	Extrusion system driven by air pump Compressive pressure (600 kPa), needle velocity (6 mm/s), needle diameter (0.58 mm), and infill density (50%)	NA	Printed dough	Liu, Meng, et al. (2019)
Dough (wheat flour, water, and ground larvae of yellow mealworms, *Tenebrio molitor*)	Wheat flour: mealworm powder (90:10 and 80:20)	Tinkercad, CURA 15.04.2	3D Printer model (Delta 2040, Wasp project, Italy, and Clay extruder kit 2.00, Wasproject, Italy)	CE	Syringe type Infill density (15%), layer height (0.5 mm), nozzle size (0.84 mm), print speed (30 mm/s), and travel speed (50 mm/s)	Baking (at 200 °C for 22 min)	Printed snacks	Severini, Azzollini, et al. (2018)
Dough (wheat flour, water, extra virgin olive oil, and sodium chloride)	Wheat flour (62%), water (31%), olive oil (6%), and sodium chloride (1%)	Tinkercad, CURA ver. 3.3.1	Delta 2040 equipped with a clay extruder kit 2.0-Wasp Project, Italy	CE	Screw driven by stepper motor Nozzle size (0.84 mm), filament diameter (1.0 mm), layer height (0.7 mm), shell thickness (0.84 mm), flow parameter (100%), print speed (200 mm/s), travel speed (200 mm/s), infill density (20%), retraction distance (1 mm) and retraction speed (105 mm/s)	Oven cooking (at 180 °C for 18 min)	Printed cereal-based snack	Derossi, Husain, et al. (2020b)
Dough (wheat flour, water, olive oil, and sodium chloride)	[Wheat flour (62 g), water (31 g), olive oil (6 g), and sodium chloride (1 g)]/100 g	Tinkercad Cura ver. 3.3.1	3D printer Delta 2040 equipped with a clay extruder kit 2.0 (Wasp Project, Italy)	CE on heated plate at 70 °C	Flow (177%), infill speed (30 mm/s), layer height (0.80 mm), nozzle size (0.84 mm), print speed (22.80 mm/s), shell thickness (0.84 mm), infill density (100%), retraction speed 30 mm/s), and travel speed (30 mm/s)	Baking (at 150 °C for 18 min)	Printed cereal-based snack	Derossi et al. (2021)
Dough (wheat flour, water, and calcium caseinate)	Wheat flour (39 g), water (30 g), calcium caseinate (1.17 g), and *Lactobacillus plantarum* WCFS1	Slic3r	3D food printer (ByFlow, the Netherlands)	Room temperature CE	Syringe type Nozzle diameter (1.2 mm), print speed (5 mm/s), and infill density (30%)	Baking (at 145 °C for 6 min)	Dough structure containing probiotics	Zhang, Lou, and Schutyser (2018)
Dough (wheat flour, wheat starch, egg-white protein, and water)	NR	SolidWorks Simplify3D	X400 V3 (German RepRap GmbH, Feldkirchen, Germany)	21 ± 2 °C CE	Syringe driven by air pressure system Nozzle diameter (0.84 mm), layer height (0.84 mm), feed rate (60 mm/s), print speed (4 mm/s), and filament diameter (0.5 mm)	NA	Printed structures	Fahmy, Becker, and Jekle (2020)
				25 °C CE		N/A	Printed gels	

(*continued*)

Table 1. Continued.

Material composition	Optimized/printable ink formulation	3D model source/ slicing software	3D Printer used and structural configuration	Printing temperature and classification of 3DFP	Extrusion mechanism and optimal printing parameters	Post-processing operation	Product	Reference
Grain gels (black rice, brown rice, job's tear seeds, buckwheat, mung bean, and water)	Steamed gels [buckwheat and black rice powders: water (1:3)]	Repetier-Host V2.0.5 Rhinoceros 5.0	SHINNOVE-D1 3D food printer (Shiyin Co., Ltd., Hangzhou, Zhejiang, China)		Syringe type Extrusion rate (35 mm^3/s), nozzle diameter (1.2 mm), and nozzle speed (20 mm/s)			Guo, Zhang, and Devahastin (2020a)
Paste (barnyard millet (BM), fried gram (FG), green gram (GG), ajwain seeds (AS), salt, red chili powder, and water)	[Flour (42% BM, 42% GG, 14% FG, 2% AS): water, 1.2:1]	NS	Delta configuration. Fabricated extrusion-based 3D printer CARK	Room temperature CE	Syringe driven by air pressure pump Print speed (2400 mm/min), nozzle diameter (0.84 mm), extruder motor speed (300 rpm), infill density (100%), and nozzle height (0.63 mm)	Hot air drying (at 100 °C for 20 min)-deep frying (165 ± 5 °C), and microwave drying (at 1400 W for 15 min)	Printed fiber and protein-rich snack	Krishnaraj et al. (2019)
Confectionery								
Breakfast spreads (vegemite and marmite)	Vegemite and marmite	Repetier-Host SolidWorks Slic3r LinuxCNC	BioBot 1 extrusion printer, BioBots	25 °C CE	Syringe driven by pneumatic pressure	NA	Printed strictures	Hamilton, Alici, and In Het Panhuis (2018)
Milk chocolate buttons	Tempered chocolate	Java program ChocALM	ChocALM system (University of Exeter)	CE	Screw type Nozzle diameter (1.25 mm), nozzle height (2.9 mm), extrusion rate (253), and axis movement rate (253)	NA	Printed chocolate	Hao et al. (2010)
Dark cooking chocolate	Melted chocolate	Repetier-Host	Cartesian design ORD Bot Hadron mechanical platform, RepRap Project	Room temperature CE	Syringe type driven by stepper motor Nozzle diameter (1.37 mm), movement speed (500 mm/min), and extrusion rate (10%–20%)	NA	Printed chocolate	Lanaro et al. (2017)
Chocolate based inks (cake icing, cocoa powder, chocolate sirup, hazelnut chocolate spread)	Chocolate sirups and pastes containing cocoa powders (10 to 25 wt/wt%)	MuCAD V, Slic3r	3D printing robot and a dispenser (SHOTmini 200 Sx and IMAGE MASTER 350 PC Smart, Musashi Engineering Inc., Japan)	Room temperature CE	Syringe type Applied pressure drop (150 kPa), layer height (0.40 mm), nozzle diameter (0.60–0.70 mm), and rate of mass flow (4.6 mg/cm)	NA	Printed chocolate	Karyappa and Hashimoto (2019)
Chocolate [dark chocolate buttons (DCB) and magnesium stearate (MGS)]	5 g of MGS per 100 g of grated chocolate	Tinkercad Repetier, Slic3r	PORIMY 3D chocolate printer (PORIMY, Kunshan, China)	32 °C CE	Screw type driven by stepper motor Nozzle diameter (0.8 mm), nozzle size (1.5 mm), and printing speed (70 mm/s)	NA	Printed chocolate	Mantihal et al. (2017)
Dark chocolates buttons	Grounded and melted chocolates	Tinkercad Repetier-Host Slic3r	Shinnove 3D printer (model no. Shinnove-D1, Shiyin Co. Ltd, Hangzhou, China)	32 °C CE	Syringe type driven by stepper motor Nozzle diameter (0.78 mm), print speed (70 mm/s), infill density (25%)	NA	Printed chocolate	Mantihal, Prakash, and Bhandari (2019a)
				32 °C CE		NA	Printed chocolate	

Chocolates (dark chocolate, DCB, MGS and plant sterol (PS) powders)	For DCB: 5% MGS or 3% PS per 100 g of grounded and melted chocolate	Tinkercad Repetier-Host Slic3r	3D chocolate printer, PORIMY 1.0 (PORIMY, Kunshan, China)		Screw type driven by stepper motor Print speed (70 mm/s), nozzle diameter (0.78 mm), and infill density (60%)			Mantihal, Prakash, and Bhandari (2019b)
Chocolates (dark chocolate, dark chocolate bittersweet flavor, MGS, and PS powders)	5 g of MGS or 3 g of PS per 100 g of grated chocolate buttons	Tinkercad Repetier, Slic3r	PORIMY 3D chocolate printer (PORIMY, Kunshan, China)	32 °C CE	Screw type Print speed (70 mm/s) and nozzle diameter (0.78 mm)	NA	Printed chocolate	Mantihal et al. (2019)
Egg and egg products								
Egg fraction paste (egg white/yolk, maltodextrin, rice flour, pepper, cumin, and water)	[Egg white powder (12.5%), egg yolk powder (54.17%), and rice flour (33.33%)]/wt/wt, 5% maltodextrin, water, ground pepper, and cumin)	Simplify3D	In-house fabricated extrusion-based delta type 3D printer	CE	Syringe type driven by pneumatic pressure Print speed (800 mm/min), nozzle diameter (1.22 mm), extrusion rate (0.0123 cm^3/s), and motor speed (180 rpm)	Steaming (> 100 °C for 5 min) and baking (540 W for 4 min)	Printed egg	Anukiruthika, Moses, and Anandhara makrishnan (2019)
Egg fraction paste (egg white/yolk, maltodextrin, and rice flour)	Egg yolk: rice flour (1:2 wt/wt), and maltodextrin (5%)	NS	Delta configuration 3D printer CARK	25 °C CE	Syringe type driven by pneumatic pressure Nozzle diameter (0.84 mm), printing speeds (600 and 800 mm/min), motor speed (180 rpm), and extrusion rate (0.005 cm^3/s)	NA	Printed egg fraction	Anukiruthika, Moses, and Anandhara makrishnan (2020)
Mixture system (egg white protein (EWP), cornstarch, gelatin, sucrose, and water)	Cornstarch (21 g), gelatin (15 g), sucrose (9 g), EWP (5% wt/wt of 300 g), and water	NS	3D printer (Kunshan PORIMY 3D Printing Technology Co., Ltd. Jiangsu Province, China)	40 °C CE	Screw system driven by stepper motor Extrusion rate (0.004 cm^3/s), nozzle height (3.0 mm), nozzle diameter (1.0 mm), and nozzle moving speed (70 mm/s)	NA	Printed product	Liu, Meng, et al. (2019)
Mixture system (cornstarch, EWP, gelatin, and sucrose, and water)	Cornstarch (19.72 g), gelatin (14.27 g), sucrose (8.02 g), EWP (12.98 g), and water (250 mL)	NS	3D printer (Kunshan PORIMY 3D Printing Technology Co., Ltd. Jiangsu Province, China)	40 °C CE	Screw system driven by stepper motor Extrusion rate (0.004 cm^3/s), nozzle diameter (1.0 mm), nozzle height (3.0 mm), and nozzle moving speed (70 mm/s)	Microwave oven (for 3 min)	Printed object	Liu, Zhang, Wei, et al. (2020)
Egg yolk paste (hen eggs)	Heat-induced egg yolk paste at 76 °C for 8 min	Rhino 5.0	SHINNOVE-E1, SHIYIN Technologies Co. Ltd., Hangzhou, China.	25 °C (CE)	Syringe type Infill density (10%), layer height (0.8 mm), nozzle height (1 mm), nozzle diameter (0.84 mm), print speed (40 mm/s), and retraction speed (50 mm/s)	NA	Printed object	Xu, Zhang, et al. (2020)

(*continued*)

Table 1. Continued.

Material composition	Optimized/printable ink formulation	3D model source/ slicing software	3D Printer used and structural configuration	Printing temperature and classification of 3DFP	Extrusion mechanism and optimal printing parameters	Post-processing operation	Product	Reference
Fish and fish products								
Purees (canned tuna, beetroot, and butternut pumpkin)	Butternut pumpkin (400 g), beetroot (400 g), and canned tuna (425 g)	Solidworks Bioplotter software	EnvisionTEC GmbH Bioplotter (EnvisionTEC, Gladbeck, Germany)	20 °C CE	Syringe type Nozzle size (0.50 mm), pressure (0.2 and 0.3 bar), and print speed (20, 25 and 40.2 mm/s)	NA	Printed tuna fish	Kouzani et al. (2017)
Surimi gel (surimi mince and NaCl)	Surimi mince and NaCl (1.5 g/100 g or 1.5% wt/wt)	Java program	NS	25 °C CE	Screw type driven by stepper motor nozzle movement speed (28 mm/s), nozzle diameter (2.0 mm), extrusion rate (0.003 cm^3/s), and nozzle height (5.0 mm)	NA	Printed *surimi* gel	Wang et al. (2018)
Surimi paste (conventional surimi, pH-shift surimi, and NaCl)	Thawed cod surimis and NaCl	Natural machines	Foodini 3D food printer (Natural Machines, Barcelona, Spain)	25 °C CE	Nozzle size (4 mm)	Steaming (at 90 °C for 20 min)	Printed surimi	Gudjónsdóttir, Napitupulu, and Kristinsson (2019)
Surimi gel (*Scomberomorus niphonius* surimi, microbial transglutaminase, NaCl, and cold water)	Surimi, NaCl (2.5% wt/wt), cold water (15%) and microbial transglutaminase (0.2% and 0.3%)	Repetier-Host V0.95F	FPE2, Fuqifan electromechanical technology Co.Ltd., Shanghai, China	20 °C CE	Syringe type Printing speed (20 mm/s), nozzle diameter (1.0 mm), and extrusion rate (15 mm^3/s)	Cooking (heating at 40 °C for 60 min and at 90 °C for 20 min)	Printed *surimi* gel	Dong, An, et al. (2020)
Fruit and vegetables								
Carrot pulp gel (Carrot, potato starch, xanthan gum, and water)	[Carrot and 50% water (545.05 and 471.17 µm), potato starch (20%), and XG (0.8%) wt/wt]	Slic3r	Shiyin Co. Ltd, Hangzhou, China	CE	Nozzle diameter (0.8 mm), and printing speed (25 mm/s)	NA	Printed carrot pulp gel	Feng et al. (2021)
Fruit based formulation (banana, canned white beans, died mushrooms, dried nonfat milk, lemon juice, ascorbic acid, and pectin powder)	Ascorbic acid (0.5%), banana (73.5%), canned white beans (15.0%), dried mushrooms (2.0%), dried nonfat milk (6.0%), lemon juice (3.0%), and pectin solution (11%)	Tinkercad CURA 14.7	Delta 2040 (Wasp project, Italy) equipped with the Clay extruder kit2.00 (Wasproject, Italy).	25 °C CE	Stainless piston chamber driven by stepper motor Nozzle size (0.84 mm), flow level (130%) and print speed (70 mm/s), layer height (0.60 mm), infill density (25%), shell thickness (0.84 mm), filament diameter (1.75 mm), and travel speed (30 mm/s).	NA	Printed snacks	Derossi et al. (2018)
Gel (lemon juice and potato starch)	Steamed gels (lemon juice and 15 g/ 100 g of potato starch)	NS	NS	25 °C CE	Screw type driven by stepper motor Nozzle diameter (1 mm), print speed (30 mm/s), and extrusion rate (24 mm^3/s)	NA	Printed gel	Yang, Zhang, Prakash, et al. (2018)
Gel (lemon juice, corn starch, potato starch, sweet	Cooked gels [Lemon juice and 15 g/ 100 g of starches]	Repetier-Host V2.0.5, Rhinoceros 5.0 Slic3r	Shiyin Co. Ltd, Hangzhou, China	25 °C CE	Syringe type driven by stepper motor Nozzle diameter (1 mm),	NA	Printed product	Yang, Zhang, Fang, et al. (2019)

potato starch, and wheat starch)					print speed (30 mm/s), extrusion rate (24 mm^3/s), and filling rate (90%)			
Gel (carrot cell dispersion and sodium alginate solution)	Cured gel [Carrot cell dispersion: sodium alginate solution (1:1 and 1:2)]	Cura 2.4	YL-R1; YOLILO, Seoul, Korea)	Room temperature CE	Syringe type Nozzle diameter (1.0 mm), layer height (0.9 mm), nozzle speed (20 mm/s), and infill density (60%)	NA	Printed product	Park, Kim, and Park (2020)
Gel (concentrated mango juice and potato starch)	Mango juice: potato starch (86.96:13.04 wt/wt)	Java program	SHINNOVE-D1, Shiyin Tech Co. Ltd., Hangzhou, China	30 °C CE	Syringe type driven by stepper motor Nozzle moving speed (25 mm/s), nozzle diameter (1.0 mm), and layer height (1.0 mm)	Microwave vacuum drying (at 150 W for 4 min)	Printed juice gel	Yang, Zhang, Fang, et al. (2019)
Smoothies (pears, carrots, kiwi fruit, avocado, broccoli raab leaves, and fish collagen)	Paste [Avocado (1.5%), broccoli raab leaves (10.0%), carrots (36.5%), kiwi (7.0%), pears (45.0%), and fish collagen (1%)]	Tinkercad CURA ver. 14.7	Delta 2040 (Wasp project, Italy) equipped with the Clay extruder kit 2.00 (Wasproject, Italy)	CE	Syringe type driven by stepper motor Nozzle size (1.2 mm), infill density (25%), shell thickness (1.2 mm), flow level (101.4%), print speed (10.97–20.77 mm/s), retraction speed (20 mm/s), travel speed (20 mm/s), and layer height (1.1 mm)	NA	Printed smoothie	Severini, Derossi, et al. (2018)
Dispersed-ink system (spinach powder, xanthan gum (XG), water)	Spinach powder (20 g/100g, 307 µm), XG (8 g/100 g), and water (72 g/100 g)	Cura 2.4	YL-R1, YOLILO Co., Ltd., Korea	25 °C CE	Syringe types Nozzle diameter (1 mm) print speed (20 mm/s), height of the first layer (0.8 mm), and height between the layer and the layer (0.7 mm).	NA	Printed spinach dispersion	Lee et al. (2019)
Pureed vegetables [Carrot, garden pea, bok choy, locust bean gum (LG), kappa carrageenan (KC), and xanthan gum (XG)]	Carrot ink (90% water content and 0.3% XG). Garden pea (80% water content). Bok Choy (96% water content, 1.0% XG, and 1.0% LBG)	SolidWorks	FOODINI (Natural machines, Spain) and Wiiboox Sweetin chocolate printer (Wiiboox, China)	Room temperature CE	Nozzle size (0.84 mm and 1.5 mm), printing speed (25 mm/s), layer height (0.5 mm), infill density (85%), and flow rate (80%)	NA	Printed vegetable inks	Pant et al. (2021)
Tomato pellet paste (tomato puree, spreads, and mayonnaise)	Concentrated tomato paste	Slic3r	ByFlow 3D printer (byFlow B.V., the Netherlands)	Ambient temperature CE	Syringe type Nozzle diameter (0.8 and 1.2 mm), print speed (18 and 25 mm/s), and layer height (0.6 mm)	NA	Printed tomato pellet paste	Zhu, Chen, et al. (2019)
Fortified fruit concentrate (orange fruit concentrate, wheat starch, vitamin D, guar gum, gum Arabic, κ-carrageenan gum, and xanthan gum)	Steamed mixture [orange fruit concentrate (100 g), wheat starch (15 g), vitamin D (1 mL), and κ-carrageenan gum (1 g)]	Repiter-Host Slic3r	3D food printer (SHINNOVE-D1, Shinnove Co. Ltd., Hangzhou, Zhejiang, China)	NS	Syringe type Nozzle diameter (0.83 mm)	NA	Printed product	Azam, Zhang, Bhandari, et al. (2018)

(continued)

Table 1. Continued.

Material composition	Optimized/printable ink formulation	3D model source/ slicing software	3D Printer used and structural configuration	Printing temperature and classification of 3DFP	Extrusion mechanism and optimal printing parameters	Post-processing operation	Product	Reference
Orange leather (orange fruit concentrate and wheat starch)	Steamed mixture (orange fruit concentrate (75 g) and 20% wheat starch, wt/wt)	Repitier-Host	FSE2, Bolimai Co. Ltd. Kunshan, China	25 °C CE	Screw type Nozzle moving speed (35 mm/s), nozzle diameter (1.5 mm), layer height (1.54 ± 0.02 mm), and extrusion rate (245 mm^3/s)	NA	Printed object	Azam, Zhang, Mujumdar, et al. (2018)
Hydrocolloid/Hydrogel								
Natural gel (potato starch, fresh or *Nostoc sphaeroides* powder)	Rehydrated *N. sphaeroides* powder (1 g in 20 mL water) and potato starch (40 g/kg)	Repetier-Host V1.06	Model FSE 2, Kunshan Bolimai Three-Dimensional Printing Technology Co. Ltd, Kunshan City, Jiangsu Province, China)	27 ± 3 °C CE	Screw type driven by stepper motor Nozzle diameter (2 mm) and nozzle height (3 mm)	NA	Printed biomass gel	An et al. (2019)
Hydrocolloid pastes (agar, gum Arabic, carrageenan, gellan gum, gelatin, guar gum, iota-carrageenan, isomalt, lecithin, locust bean gum, maltodextrin, methylcellulose, pectin, sodium alginate, xanthan gum, and water)	Gelatin (2% wt/vol)	Cura15.04.6	Custom-built food 3D printing system	Room temperature CE	Syringe type 22 G needle diameter (0.413 mm), 18 G needle (0.838 mm), pipette tip (0.52 mm), and flow level (40%–100%)	NA	Printed gel pastes	Gholamipour-Shirazi, Norton, and Mills (2019)
Gel (κ-carrageenan and water)	30 mg/g of κ-carrageenan in water	AutoCAD, Tinkercad, Cura, Repsetier-Host	BQ Hephestos 3D printer DIY kit, with Marlin-derived firmware designed by BQ (Spain)	80–85 °C HE	Syringe type Nozzle diameter (0.4 mm), layer height (0.06, 0.11, 0.18, 0.25, and 0.30 mm) and print speed (10, 20.1, 35.0, 49.9, and 60 mm/s)	NA	Printed gel	Diañez et al. (2019)
Gel [Xanthan gum, gelatin, water, and flavor concentrates (banana, chocolate, raspberry, and strawberry)]	4% gelatin	Fab@Home control software	Fab@home	NR	Syringe type	NA	Printed gel	Cohen et al. (2009)
Gels (Glucomannan (KGM), sugar sirup, xanthan gum, calcium gluconate anhydrous (CGA), Calcium lactate hydrate (CLH), and water)	KGM (0.0165), sugar sirup (0.9773) and xanthan gum (0.0062) [Water (100 mL), sugar (20 g), CLH/CGA (2 g), and 1 µg colorant]	Tinkercad Slic3r	Commercial 3D printer (BCN 3D+, BCN3D Technologies, Barcelona, Spain)	50 °C, CE-HE	Syringe type Nozzle diameter (2.0 mm), print speed (15 mm/s), nozzle height (2 mm), and flow rate (70 mm^3/s)	NA	Printed gel	García-Segovia et al. (2020)

Hydrocolloid mixtures (agar, gelatin, gellan gum, guar gum, hydroxypropyl methylcellulose, locust bean gum, methylcellulose, water, and xanthan gum)	Concentration range (1%–20% wt/wt)	Cura 2.4	Custom built food 3D printing system, Korea University	25 °C CE	Nozzle diameter (1.1 mm), print speed (20 mm/s), and layer height (0.9 mm),	NA	Printed product	Kim, Bae, and Park (2018)
Gels (low methoxylated (LM) pectin, bovine serum albumin (BSA), $CaCl_2$, sugar sirup, and water)	LM pectin (55 g/L), $CaCl_2$ (12.5 mM), sugar sirup (25% vol/vol), BSA (5 g/L), and edible colorant	AutoCAD Slic3r	3-D robotic system (CNC Bench 3D 4046, GoCNC.de, Germany)	Room temperature CE	Syringe type Nozzle diameter (0.838 mm), flow rate (0.34 mL/min), layer height (0.838 mm), infill velocity (10 mm/s), infill density (85%), and travel velocity (200 mm/s)	Incubation (in 300 mM $CaCl_2$ for 10 min) and spraying (with 300 mM calcium solution for 90 min)	Printed gels	Vancauwenberghe et al. (2017)
Gels (LM pectin, $CaCl_2$, and water)	LM pectin (15 and 35 g/L) and $CaCl_2$ (10 and 15 mM)	AutoCAD Slic3r	CNC robotic system (CNC Bench 3D 4046, GoCNC.de, Germany)	NS	Syringe type Nozzle diameter (0.84 mm and 1.2 mm), flow rate (0.1, 0.3, 0.34, and 0.5 0 mL/min), layer height (0.85 mm), infill velocity (10 mm/s), infill density (85%), and travel velocity (200 mm/s)	NA	Printed product	Vancauwenberghe, Verboven, et al. (2018)
Gels (LM pectin, $CaCl_2$, and water)	LM pectin (25 g/L), $CaCl_2$ (12.5 mM), and red food colorant (2 drops)	AutoCAD Slic3r	3D robotic system (CNC Bench 3D 4046, GoCNC.de, Germany)	23 °C CE	Syringe pump Flow rate (0.34 mL/min), infill density (85%), layer height (0.84 mm), infill velocity (10 mm/s), travel velocity (200 mm/s), and nozzle diameter (0.84 mm)	Incubation (in 50 mM $CaCl_2$ solution for 60 min)	Printed structures	Vancauwenberghe, Delele, et al. (2018)
Gel formulation (xanthan gum, κ–carrageenan, potato starch, food color, and water)	κ–carrageenan (1% wt/wt), potato starch (2 % wt/wt), xanthan gum (0.5% and 0.25% wt/wt), and food color (0.1%)	Rhinoceros 5.0 Skeinforge	3D printer (Choc Creator 2.0 Plus, Choc Edge Co. Ltd, UK)	40 °C CE	Syringe type Feed rate and print rate (22 mm/s), nozzle diameter (0.8 mm), solid infill, and layer height (0.8 mm)	NA	Printed constructs	Liu, Meng, et al. (2019)
Casienate dispersion (sodium casienate, potato starch, olive oil, pectin, and sucrose)	NR	PathBuilder version 3.9 SketchUp 2014	Fluid dispensing robot (model 2203, Nordson EFD)	31.5, 67 and 77 °C CE-HE	Syringe type Needle diameter (1 mm) and print speed (10 and 60 mm/s)	NA	Printed structures	Schutyser et al. (2018)
Gel (gelatin and kappa-carrageenan)	NR	Repetier	Hictop Prusa i3 printer	20 °C CE	Syringe type Print speed (10 mm/s), travel speed (100 mm/s), nozzle diameter (0.6 mm), and layer height 0.3 mm	NA	Printed structures	Warner, Norton, and Mills (2019)
Gel (pea-protein powder, alginate	NR	COMSOL Multiphysics version 3.5. Cura	FDM printer (SHINNOVE-S2, Shinnove Co. Ltd.,	25 ± 1 °C CE	Syringe type Layer height (0.68 mm), nozzle diameter	NA	Printed material	Oyinloye and Yoon (2021)

(continued)

Table 1. Continued.

Material composition	Optimized/printable ink formulation	3D model source/ slicing software	3D Printer used and structural configuration	Printing temperature and classification of 3DFP	Extrusion mechanism and optimal printing parameters	Post-processing operation	Product	Reference
powder, and calcium chloride)			Hangzhou, Zhejiang, China)		(0.84 mm), and travel speed (15 mm/s)			
Polysaccharide hydrogels (gellan gum, locust bean gum, low methoxyl pectin, tara gum, xanthan gum, and water)	NR	Rhinoceros 5.0	SHINNOVE-D1 3D food printer (Shiyin Co., Ltd., Hangzhou, Zhejiang, China)	25 °C CE	Syringe type Nozzle moving speed (20 mm/s), nozzle diameter (1.2 mm), and volume extrusion rate (35 mm^3/s)	NA	Printed objects	Guo, Zhang, and Devahastin (2020b)
Legumes								
Gels (soy protein isolate powder, xanthan gum, NaCl, and water)	NR	NS	3D printing system (Shiyin Co., Ltd., Hangzhou, China)	25 ± 1 °C CE	Screw type Nozzle diameter (1.2 mm), print speed (15 mm/s), and extrusion rate (25 mm^3/s)	NA	Printed gel	Phuhongsung, Zhang, and Devahastin (2020)
Maillard reaction product (pea protein edible glycerol, Maillard reaction product of xylose–pea protein enzymatic hydrolysate, and potato starch)	NR	NS	3D printer (PORIMY Co. Ltd, Wuxi, China)	38 °C CE	Nozzle size (1.0 mm), print speed (15 mm/s), and layer height (1.0 mm)	NA	Printed product	Zhou et al. (2020)
Slurry [soybean protein isolate (SPI) powder, strawberry powder (SP), salt, and water]	SPI (4 g), SP (2 g), 20 mL saline solution (3.5% wt/vol)	NS	3D printer (SHINNOVE-D1, Shiyin Tech Co.Ltd. (Hangzhou, China)	Room temperature CE	Nozzle diameter (1.2 mm), print speed (17 mm/s), and first layer height (0.9 mm)	NA	Printed product	Fan et al. (2020)
Paste (soy protein isolate, sodium alginate, and gelatin)	NR	Cura 15.04.6	3D printer (3.0, Felix, The Netherlands)	35 °C Room temperature	Syringe type Nozzle diameter (1.55 mm), layer height (0.6 mm), flow rate (80%), print speed (10 mm/s), and infill density (0 and 100%)	NA	Printed product	Chen, Xie, et al. (2019)
Meat product								
Meat paste (beef, lard, NaCl, guar gum and water)	Minced meat (85%), water (15%), NaCl (1.5%), and guar gum (0.5%)	Tinkercad Slic3r Repetier-Host V2.1.2	Dual nozzle model 3D printer (Shinnove, Hangzhou Shiyin Technology, China)	23 ± 1 °C CE	Print speed (20 mm/s), flow rate (100%), layer height (1.95 mm), nozzle diameter (1 and 2 mm), and infill density (50, 75 and 100%)	Sous-vide cooking (at 75 °C for 30 min)	Composite multi-layer meat models	Dick, Bhandari, and Prakash (2019)
Meats purees (turkey, scallop, celery, agar, and transglutaminase)	NR	NS	Fab@Home 3d printer	NS	NS	Deep frying and slow cooking	Printed meats	Lipton et al. (2010)
Slurry (fibrous meat, gelatin powder, chicken essence,	Meat juice (chicken, fish, and pork)	NS	Developed food 3D printing system, Taiwan, University	NS	Peristaltic pump Nozzle diameter (2, 4 and 5 mm)	NA	Printed product	Liu, Ho, et al. (2018)

and liquid pork essence)	gelatin powder (20 g), water (100 g)							
Pastes (chicken, shrimp, and sesame pastes)	Sesame paste [black sesame powder, rice flour, and water(1:1:2)], chicken paste [egg white and raw chicken (300 g)], shrimp paste (raw shrimp, cooking wine (1 teaspoon), half an egg white, grated ginger, pepper powder (2 teaspoons), and rice flour (1 teaspoon)	Java applet	Custom 3D printer, Columbia University	NS	Syringe type Print speed (20 mm/s), flow rate (51.6 mm^3/s), and cooking speed (3.33 mm/s)	Infrared cooking	Printed product	Hertafeld et al. (2019)
Milk and milk products			NR					
Casein-whey protein suspension (micellar casein concentrate, whey protein isolate, citric acid, and water)	Casein (10%, pH 4.8), whey protein (2.5%, heated pH 6.9), citric acid (1M), and NaOH (1M)	Repetier	Plastic printer (Creality 196 Ender 3 Printer; Creality, Shenzhen, China)	NS	Syringe type Nozzle diameter (1.15 mm), print speed (20 mm/s), and layer height (1 mm)	NA	Printed gels	Daffner et al. (2021)
Paste (milk powder, rye bran, cellulose nanofiber, starch, water, oat and faba bean protein concentrates)	Semi-skimmed milk powder (60%), starch (10%), rye bran (30%), skimmed milk powder (15%), water, oat and faba bean protein concentrates (35% or 45%, respectively)	NS	VTT's micron scale dispensing environment based on nScrypt technology (nScrypt, Inc, Orlando, Florida)	Room temperature CE	Air syringe pump Print speed (2 mm/s), nozzle diameter (0.41 mm), and nozzle height (0.3 mm)	Oven drying (at 100 °C for 20-30 min)/ freeze drying	Printed paste	Lille et al. (2018)
Milk protein paste (milk protein concentrate, MPC), whey protein isolate (WPI), water, glycerol, and xanthan)	MPC:WPI (5:2, w/w), and solution [water and glycerol (1:1, w/w), and xanthan gum (0.5%, w/v)]	Rhino 5.0 Cura 15.0	3D printer (SHINNOVE-S2, SHIYIN Technologies Co.Ltd., Hangzhou, China)	25 °C CE	Syringe type Print speed (35 mm/s), retraction speed (50 mm/ s), nozzle diameter (0.84 mm), flow rate (100%), nozzle height (1.0 mm), filament diameter (22 mm), infill density (30%), and layer height (0.75 mm)	NA	Printed milk powder paste	Liu, Ho, et al. (2018)
Cheese	Melted cheese (75 °C for 12 min)	NS	RepRap Pro Ormerod 1 (RepRap Professional Ltd, UK)	NS	Syringe type Nozzle diameter (1.5 mm), extrusion rate (4 or 12 mL/min)	NA	Printed cheese	Le Tohic et al. (2018)
Composite gel (MPC and sodium caseinate)	MPC (400-450 g/L) and sodium caseinate	Rhino 5.0 Cura 15.0	3D printer (SHINNOVE-S2, SHIYIN Technologies Co.	NS	Syringe type Print speed (35 mm/s), nozzle diameter (0.84 mm), layer height	NA	Printed gels	Liu, Yu, et al. (2019)

(*continued*)

Table 1. Continued.

Material composition	Optimized/printable ink formulation	3D model source/ slicing software	3D Printer used and structural configuration	Printing temperature and classification of 3DFP	Extrusion mechanism and optimal printing parameters	Post-processing operation	Product	Reference
	dispersion (20%, w/v)		Ltd., Hangzhou, China)		(0.75 mm), retraction speed (50 mm/s), infill density (30%), nozzle height (1 mm), and flow rate (100%)			
Gel-like emulsion (WPI and soy oil)	Pickering emulsion [heated WPI dispersion (10%, w/v, at 70 °C for 60 min) and soy oil (0.4-0.6)]	Rhino 5.0 Cura 15.0	3D food printer (SHINNOVE-S2, Shiyin Technologies Co. Ltd., Hangzhou, Zhejiang, China)	25 °C CE	Syringe type Print speed (35 mm/s), retraction speed (50 mm/s), nozzle diameter (0.84 mm), layer's height (0.75 mm), filament diameter (22 mm), flow rate (100%), nozzle height (1.0 mm), and infill density (100%)	NA	Printed emulsions	Liu, Zhang, et al. (2019)
Root and tubers								
Cookie dough (tapioca, rice, and wheat flour, butter or shortening, sugar, and milk)	Tapioca flour (shortening, sugar, milk)	Solidworks Slic3r	Modified 3D printer (Prusa i3, Prusa Research, Prague, Czech Republic)	Room temperature CE	Syringe driven by air pressure Air pressure (2–20 psi), print speed (300 mm/min), and nozzle diameter (2.4 mm)	Baking	Printed cookie dough	Pulatsu et al. (2020)
Potato paste (purple sweet potato flour and water)	Flour: water (1:2.25, 1:2.5, and 1:2.75)	Rhinoceros 5.0 Simplify3D	SHINOVE-D1 3D food printer (Shiyin Co., Ltd., Hangzhou, China)	25 °C CE	Printing driven by stepper motor Nozzle diameter (1.2 mm), print speed (900 mm/min), and flow rate (0.149 cm^3/s)	NA	Printed paste	Chen, Zhang, Guo, et al. (2021)
Dough (potato flakes, soybean oil, wheat flour, sucrose, and NaCl)	Steamed dough (potato flakes (75 g), wheat flour (25 g), soybean oil (20 g), NaCl, and water (150 g)	NR	Shiyin Co. Ltd. (Hangzhou, China).	Room temperature CE	Nozzle diameter (1.2 mm), printing speed (25 mm/s), and infill percentage (50%)	Microwave vacuum drying (4 W/g)	Printed snack	Liu and Zhang (2021)
Potato puree (potato powder, alginate, agar, whole milk, glycerol, and lecithin)	Potato powder (115 g), milk (450 mL), water (50 mL), agar (0.5%–1%) or alginate (0.5%–1.5%)	Csura 15.02.01	RepRap BCN3D + printer (CIM Foundation)	NS	Syringe type Print speed (40 mm/s), nozzle diameter (4 mm), flow level (100%), travel speed (100 mm/s), infill speed (40 mm/s), nozzle height (0.5 cm), and retraction speed (40 mm/s)	NA	Printed product	Dankar, Pujolá, et al. (2018)
Potato puree (potato, alginate, agar, butter, carrot, and olive oil)	Potato (100 g) and butter (1% wt/wt)	Cura 15.02.01	RepRap BCN3D + extruder printer (CIM Foundation, Barcelona, Spain)	20 °C CE	Syringe type Nozzle diameter (4 mm), printing speed (40 mm/s), flow level (100%), travel speed (100 mm/s), infill speed (40 mm/s), and retraction speed (40 mm/s)	NA	Printed product	Dankar et al. (2020)

Gel (potato starch and anthocyanin powder)	Potato starch (7.5 g/ 100 mL of anthocyanin solution	SketchUp Pro2015, Slic3r	(SHINNOVED1, Shinnove Co. Ltd., Hangzhou, Zhejiang, China)	25 °C CE	Syringe type Print speed (25 mm/s), nozzle diameter (0.85 mm), and nozzle height (0.85 mm)	NA	Printed gel	Ghazal, Zhang, and Liu (2019)
Cassava starch hydrogels (cassava starch)	Dry heat-treated starch	Repetier-Host V2.0.1 Slic3r	Stampante 3D (3DRAG V1.2, Futura Elettronica, Italy)	20 °C CE	Syringe type Nozzle height (18 mm), print speed (20 mm/s), nozzle diameter (0.8 mm), and extrusion rate (30 mm/s)	NA	Printed hydrogel	Maniglia et al. (2020)
Mashed potato (gelatinized potato flakes, κ-carrageenan, and xanthan gum)	Gelatinized mixture at 70 °C for 30 min (potato flakes: water (1:4) and κ-carrageenan: xanthan gum (3:2)	Rhinoceros 5.0 Slic3r	3D printer (Shiyin Co. Ltd., Hangzhou, China)	Room temperature CE	Syringe type Nozzle diameter (0.8 mm), print speed (25 mm/s), infill levels (10%–100%), and layer height (0.8 mm)	NA	Mashed potato construct	Liu, Bhandari, et al. (2018)
Mashed potatoes (gelatinized potato flakes, κ-carrageenan gum, guar gum, and xanthan gum)	Mashed potatoes at 70 °C for 30 min (potato flakes: water (1:4) and 1% w/w of κ-carrageenan: xanthan gum (3:2)	Repetier-Host Slic3r	3D printer (CSE 1, BolimaiCo. Ltd., Kunshan, China)	NS	Screw-type Nozzle diameter (1.0 mm) and pretest condition	NA	Printed product	Liu, Zhang, and Bhandari (2018)
Mashed potatoes/ strawberry juice gel (Potato flakes, strawberry juice, potato starch, κ-carrageenan, and xanthan gum)	Mashed potato at 70 °C for 30 min (potato flakes: water (1:4) and 1% w/w of κ-carrageenan: xanthan gum (3:2); Strawberry juice gel [steam cooked (at 97 °C for 20 min) potato starch (17.5 g) and strawberry juice concentrate (100 g)]	Rhinoceros 5.0 Slic3r	Two nozzle 3D printer (Shiyin Co. Ltd, Hangzhou, China)	25 °C CE	Syringe type Print speed (25 mm/s), layer height (1.2 mm), and infill level (40%–100%)	NA	Printed product	Liu, Zhang, and Yang (2018)
Mashed potatoes (potatoes and native potato starch)	Steam cooked mix at 97 °C for 20 min (potatoes, trehalose 15% w/ w, and potato starch 2%)	Repetier-Host	3D printer (FSE2, Bolimai Co.Ltd, Kunshan, China)	25 °C CE	Screw type Nozzle diameter (2 mm) and nozzle height (3.0 mm)	NA	Printed product	Liu, Zhang, and Bhandari (2018)
Mashed potato (potato flakes and water)	Potato flakes and water (1:3)	Repetier-Host V2.0.5 Slic3r	Polar configurations. 3D printers (screw type - SHINNOVE-D1, Shiyin co. LTD, Hangzhou, China) (syringe type - FSE 2, PORIMY co. LTD, Wuxi, China)	26 °C CE	Screw and syringe types driven by steeper motors Nozzle diameter (1.0 mm)	NA	Printed product	Guo, Zhang, and Bhandari (2019a)
Potato puree (dehydrated	Dehydrated potato puree (38 g) and	Tinkercad Slic3r	Cartesian configuration. 3D printer (BCN 3D+,	30 °C CE	Syringe type Nozzle diameter (2.0 mm), nozzle height	NA	Printed product	Martínez-Monzó, Cárdenas, and

(continued)

Table 1. Continued.

Material composition	Optimized/printable ink formulation	3D model source/ slicing software	3D Printer used and structural configuration	Printing temperature and classification of 3DFP	Extrusion mechanism and optimal printing parameters	Post-processing operation	Product	Reference
potato puree and whole milk)	whole milk (250 mL)		BCN3D Technologies, Barcelona, Spain)		(1 and 2 mm) and extrusion speed (15 and 30 mm/s)			García-Segovia (2019)
Mashed potatoes (potato flakes, xanthan gum (XG), milk, kappa-carrageenan (KG), and *Bifidobacterium animalis* subsp. *Lactis* BB-12	Milk: potato flake (4.5:1), KG:XG (3:2), and probiotic powder (2%)	Rhinoceros 5.0	Two nozzle 3D printer (Shiyin Co. Ltd, Hangzhou, China)	25, 35, 45, and 55 °C CE/HE	Metal syringe driven by stepper motor Nozzle diameter (1.0 mm), Infill level (100%), and nozzle movement rate (20 mm/s)	NA	Printed mashed potatoes	Liu, Bhandari, et al. (2020)
Potato slurry (potato flakes, wheat flour, water, and bovine fat)	Potato flakes (75 g), wheat flour (25 g), fat (25 g), and water (200 g)	Rhinoceros 5.0	3D printer (Shiyin Co. Ltd., Hangzhou, China)	45 °C CE	Syringe type Print speed (25 mm/s), layer height (1.2 mm), and infill level (30, 50, and 70%)	Air frying (140 °C for 12, 16, and 21 min)	Printed potato snack	Liu, Dick, et al. (2020)
Mashed potatoes (potato flakes, water, and anthocyanin)	Water: potato flakes (2.5:1, 3.0:1, 3.5:1, and 4.0:1)	Rhinoceros 5.0 Slic3r	3D printer (Lingfeng Agricultural Products Development Co., Ltd, Hebei, China)	25 °C CE	Syringe type driven by stepper motor Infill level (0%) and nozzle diameter (1.2 mm)	NA	Printed structure	Liu, Zhang, and Ye (2020)
Paste (taro flour, guar gum, sodium carboxymethyl cellulose, sodium alginate, xanthan gum, and whey protein)	Steam cooked paste [taro flour: water (1:4, w/w) and sodium alginate (1%, w/w)]	Repetier-Host	3D printer(SHINNOVE-D1; Shiyin Technology Co., Ltd., Hangzhou, China)	25 °C CE	Extrusion rate (13 mm^3/s), nozzle diameter (0.84 mm), and print speed 25 mm/s	NA	Printed object	Huang et al. (2020)
Paste (water, dried yam, and potato processing by-product (PP) powders)	Yam: PP (7:3), 400 g/L of water	Rhino 6.0, Simplify3D	Dual nozzle 3D printer (SHINNOVE-D1, Hangzhou Shiyin Technology Co., Ltd, Zhejiang, China)	Room temperature CE	Print speed (20 mm/s), nozzle diameter (1.2 mm), layer height (1.2 mm), extrusion rate (22 mm^3/s), and Infill level (20%–80%)	Air frying (130 °C for 12, 16, and 24 min)	Printed Snacks	Feng et al. (2020)
Mashed potatoes (potato flakes, purple sweet potato puree, citric acid, sodium alginate, and sodium bicarbonate)	Mashed potatoes (potato flakes and citric acid)	Repetier-Host V2.1.3 Rhinoceros 5.0 Slic3r	3D food printer (Shiyin Co. Ltd., Hangzhou, China)	NS	Syringe type Layer height (1.2 mm), nozzle diameter (1.2 mm), and printing rate (15 mm/s)	NA	Printed products	He, Zhang, and Guo (2020)
Starch								
Gel (Buckwheat starch, high-methoxy pectin, calcium chloride, and water)	Buckwheat starch, pectin, 1% calcium chloride, and water	Repetier Host 2.0.5	FOODBOT-MF printer (Shiyin Co., Ltd., Hangzhou, Zhejiang, China).	25 °C CE	Nozzle diameter (0.8 mm), printing speed (20 mm/s), and extrusion rate (35 mm^3/s)	NA	Printed gels	Guo, Zhang, and Devahastin (2021)

Starchy gels [tapioca dextrin (TD), waxy maize starch (WMS), sugar, liquid colorants, and water)	[(TD 30 g, WMS 10 g, sugar 10 g, water 44.7 g, and yellow colorant 0.3 g)/100 g]	Rhinoceros 6 Pronterface	TNO in-house manufactured 3D printer	25, 35, and 45 °C CE	Syringe driven by stepper motor Nozzle diameter (1 mm), layer height (0.8 mm), extrusion speed (300 mm/min), and printing speed (900 mm/min)	NA	Printed gels	Paolillo et al. (2021)
Gel (cassava starch)	Starch ozonated for 30 min and stored for 7 days	Repetier-Host V2.0.1 Slic3r	3D printer Stampante 3D (3DRAG V1.2, Futura Elettronica, Italy)	20 °C CE	Syringe type Nozzle height (18 mm), nozzle diameter (0.8 mm), extrusion rate (30 mm/s), and print speed (20 mm/s)	NA	Printed gels	Maniglia et al. (2019)
Starch suspensions (corn, potato, and rice starches)	NR	NS	HE-3D printer SHINNOVE S2 (Shiyin Tech Co., Ltd., Hangzhou, China)	70–85 °C, HE	Feed cylinder driven by stepper motor Nozzle; diameter (0.8 mm), height (2.0 mm), print speed (20 mm/s), and extrusion rate (30 mm/s)	NA	Printed starch	Chen, Xie, et al. (2019)
Suspension (Potato starch and water)	NR	NS	SHINNOVE-S2 printer (Shiyin, China).	70 °C HE	Nozzle diameter (0.8 mm), nozzle height (1.0 mm), nozzle speed (30 mm/s), pulling rate 50 mm/s), and pulling distance (2 mm)	NA	Printed gel	Liu, Chen, et al. (2020)
Paste suspension (wheat starch, papaya powder, and water)	Suspension treated with ultrasound at 30 kHz for 30 min and microwaved at 80 W for 4 min	Repetier-Host Slic3r Rhino 5.0	SHINNOVE-D1, Shiyin Technologies Co. Ltd., Hangzhou, China	25 °C CE	Layer height (1.0 mm), nozzle diameter (1.0 mm), and print speed (15 mm/s)	NA	Printed object	Xu, Zhang, et al. (2020)
Dough-like (rice starch and water)	NR	Simplify3D	Delta model 3D printer CARK	Room temperature CE	Syringe type Infill level (100%), nozzle diameter (1.5 mm), and print speed (1500 mm/min)	NA	Printed construct	Theagarajan, Moses, and Anandha -ramakrishnan (2020)
Multi-food class								
Gel, paste, dough, among others (Cookie dough, cream cheese, gelatin, instant mashed potato, miso, no-meat mince, rice starch gel, peanut butter, pea protein paste, sausage meat, and wheat starch)	Cookie dough, cream cheese, and instant potato mash	SolidWorks Slic3r	Custom-built 3D printer	20, 26, 60, and 80 °C CE-HE	Syringe type Nozzle diameter (0.83 mm and 1.50 mm), layer height (0.6 mm and 1 mm), print speed (10 mm/s), and fill density (100%)	NA	Printed food inks	Nijdam, Agarwal, et al. (2021)
		NR		Room temperature CE		NA	Printed gel system	

(continued)

Table 1. Continued.

Material composition	Optimized/printable ink formulation	3D model source/ slicing software	3D Printer used and structural configuration	Printing temperature and classification of 3DFP	Extrusion mechanism and optimal printing parameters	Post-processing operation	Product	Reference
Pastes [Protein matrix (casein, peanut protein isolate, pea protein isolate, wheat hydrolyzed protein, whey protein isolate), fruit and vegetable powders (lemon powder, hawthorn powder, potato starch, and spinach powder), and sodium alginate]	Peanut protein isolate based ink: water (3:5)		FOODBOT-MF, China Changxing Shiyin Technology Co., Ltd		Syringe type Nozzle diameter (0.8 mm), printing speed (1200 mm/min), and infill rate (30%)			Chen, Zhang, Guo, et al. (2021)

CE, cold extrusion; HE, hot extrusion; NA, not applicable; NR, not reported; NS, not specified.

grade additives functioning as a binding agent are usually incorporated to achieve desirable viscosity and rheological property, supporting the ease of extrusion and printed structure post-deposition (Derossi et al. 2018; Kim et al. 2019). However, this does not suggest printing other materials without a binding mechanism is impossible, as briefly highlighted and demonstrated in available studies (Table 1). Examples of such food formulas are high fiber containing protein composite flour paste, rice dough, and insect-enriched wheat dough (Severini, Azzollini, et al. 2018; Krishnaraj et al. 2019; Liu, Tang, Duan, Qin, Zhao, et al. 2020).

The printability of those products was significantly attributed to the synergistic interaction between macromolecules, wherein (a) re-distribution of starch components might have contributed to the shear-thinning characteristic of the printable substrates (b) the degree of moisture-starch cross-linking polymerization could have led to a sufficient fluidity and formability of the inks relatively to a balance between their elastic solid-like, and viscous behaviors (c) moderate level of fat could function as a lubricant during printing or the solid form could chemically interact with starch polymers, and (d) complex interactions between different proteins may produce softer ink with printable rheological properties. For instance, during the printing of rice inks containing higher amylose fractions, defects such as broken lines of extrusion and fragile filament were observed (Liu, Tang, Duan, Qin, Zhao, et al. 2020). In contrast, high amylopectin rice ink with moderate apparent viscosity overcame the printability issues (Liu, Tang, Duan, Qin, Zhao, et al. 2020). Overflow of 20% enriched insect dough printing deposition influenced mismatches to the virtual model dimension, as evidence by the decreased height and increased diameter and weight of printed snacks (Severini, Azzollini, et al. 2018). Thus, it is pertinent to note that food inks' suitability for 3D printing may greatly depend on food material constituents/composition and corresponding dynamic viscosity and rheological properties, which may/may not require systematic modifications to determine sufficient ink fluidity, malleability, and mechanical strength. While the increasing level of non-fat milk and sugar contents of cookie doughs containing no stabilizers or gums resulted in increased deformability of dough samples (rice, tapioca, and wheat) and more collapse of the 3D constructs after baking, respectively (Pulatsu et al. 2020), tapioca dough with reduced sugar and milk levels gave better viscoelastic properties, supporting structurally stable 3D printed cookies. As such, the realization of a printable material may necessitate an iterative and arduous experimental approach.

3.1.2. Use of rheological data to predict material printability

Studies have also demonstrated that the printability of food ink formulation can be established based on computed rheological data (Dankar et al. 2020; García-Segovia et al. 2020). Such quantitative estimations have made it possible to determine food ink flow properties and structural behavior (Derossi, Paolillo, et al. 2020; Park, Kim, and Park 2020;

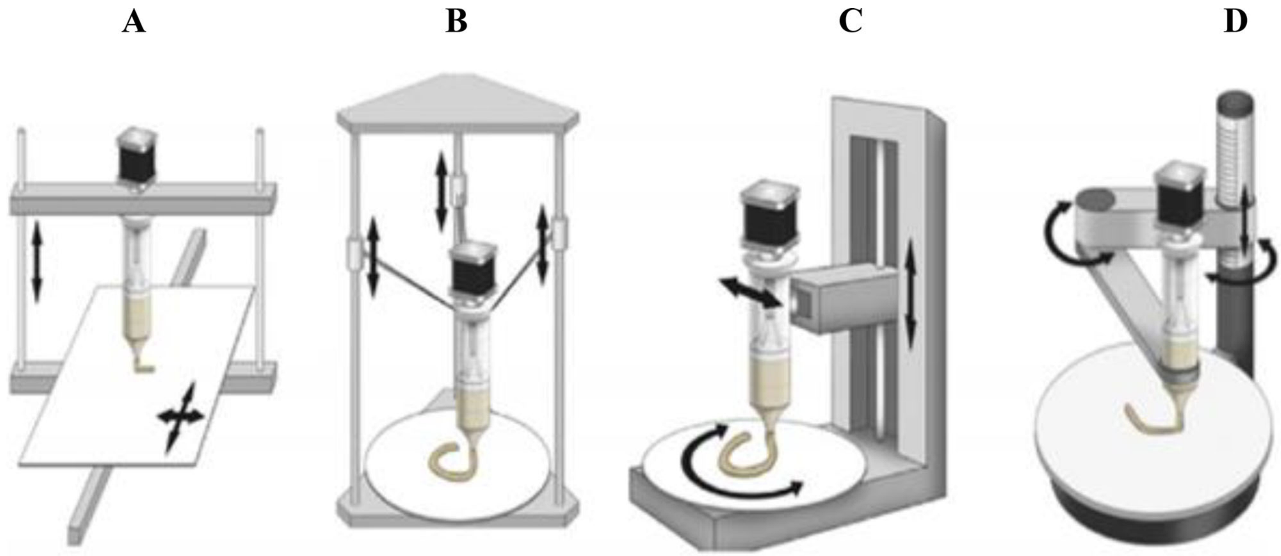

Figure 2. Structural configurations of major 3D food printers. (A) Cartesian (B) Delta (C) Polar (D) Scara (Adapted from Sun et al. 2018).

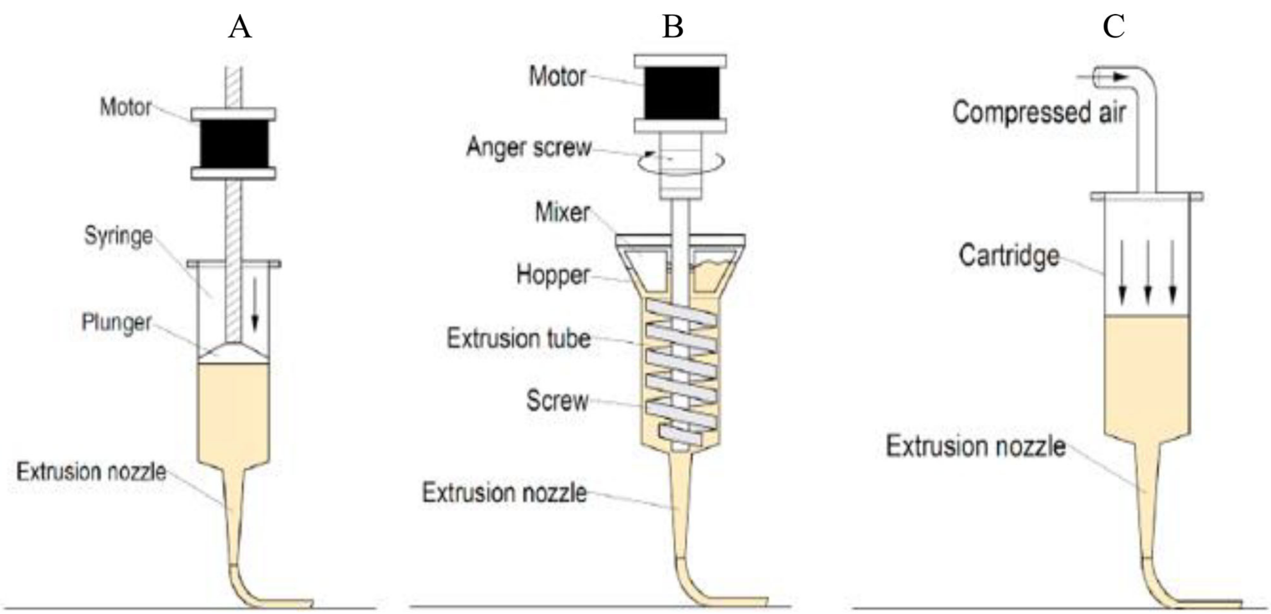

Figure 3. Types of 3D food extrusion mechanisms. (A) syringe-type extrusion (B) screw-type extrusion (C) air pressure-driven extrusion (Adapted from Guo, Zhang, and Bhandari 2019b).

Phuhongsung, Zhang, and Devahastin 2020). Appropriate food ink dynamic viscosity and viscoelastic properties are crucial for desired printability (Kim et al. 2019; Liu, Tang, Duan, Qin, Zhao, et al. 2020). The rheological results are optimally characterized based on flow behavior index, yield stress, consistency behavior index, viscosity, thixotropy, and dynamic viscoelastic properties (Ahmed, Ptaszek, and Basu 2017; Pérez et al. 2019). The non-Newtonian shear thinning characteristics depict a food material's typical flowability, undergoing extrusion, and a good match to the 3D design model (Yang, Zhang, Prakash, et al. 2018; Liu, Bhandari, et al. 2019). The shear-thinning behavior reported for high fiber containing protein composite flour paste (barnyard millet, fried gram, green gram, and ajwain seeds) (Krishnaraj et al. 2019) and rice dough (Liu, Tang, Duan, Qin, Zhao, et al. 2020), with no added binding mechanism, indicate the inks flowability and are non-Newtonian fluids preferred for 3DF printing via extrusion mechanisms.

Furthermore, the dynamic viscoelastic properties such as (a) complex modulus (G^*) is related to material rigidity, (b) storage modulus (G') describes elastic solid-like behavior, (c) loss modulus (G") reflects liquid-like or viscous behavior, while (c)/(b) estimates loss tangent (tan δ); where tan δ value greater than unity equals viscous characteristics, whereas smaller than unity interprets solid-like behavior (Liu, Tang, Duan, Qin, Zhao, et al. 2020; Chen, Zhang, Devahastin, et al. 2021). A higher G^* and G' reflects greater mechanical strength of a printing substrate; a measure of self-supporting material deposition, printing resolution, and construct dimension stability to resist compressed deformation over time (Kim et al. 2019; Feng et al. 2020; Liu, Zhang, and Ye 2020). However, too high mechanical strength may lead to printing failure due to ink occlusion at the printing nozzle tip. Thus, food ink possessing sufficient mechanical strength with appropriate shear-thinning behavior and rapid shear recovery properties are required for good printability (Paxton et al. 2017; Liu, Meng, et al. 2019).

The mechanical spectrum of rice doughs and mixed powder paste containing yam and potato processing by-product were reported to show higher G' and tan $\delta <$ unity, the preferred indices to obtain a potential solid elastic-like 3D printed construct (Feng et al. 2020; Liu, Tang, Duan, Qin, Zhao, et al. 2020). These ideal trends of viscoelastic properties are consistent with the higher G' values reported for fermented milk (Hamet, Piermaria, and Abraham 2015), fermented rice extracts showed non-Newtonian behavior (Costa et al. 2016), while shear-thinning behavior, greater G', lower tan δ were recorded for germinated Chenopodium (*Chenopodium album*) grain flour (Jan, Saxena, and Singh 2018). Several complex interactions and formation of biomolecules stimulated by the extent of the modification processes on the raw substrates could have facilitated the conforming flow behaviors and visco-elastic capacity of the resulting products. These include changes in viscosity which could be associated with the production of acids that hydrolyzes available starch into smaller molecules, exhibiting modified granule size and augmented free amylopectin chains (Costa et al. 2016), as well as the formation of exopolysaccharide and their interactions with protein network that might have influenced higher elastic modulus of acid milk gels (Hamet, Piermaria, and Abraham 2015). Accordingly, biomodified food products with compatible rheological properties hold potential consideration for desirable printability.

3.1.3. Alternative approaches to predict material printability

Moreover, actualizing the printability of a food material formulation through rheological evaluation or iterative 3D printing experiments is a time-consuming approach. Nijdam, LeCorre-Bordes, et al. (2021), in their study, developed a window of dimensional stability, a novel practical tool for rapidly screening potential edible inks based on appropriate rigidity (rheology) or estimate suitable structural heights of printed constructs for adequate dimensional stability. Nijdam, Agarwal, et al. (2021) conducted the screening method's applicability using varying food inks representing a broad range of rheological properties. The authors inferred that experimented food inks such as cookie dough, cream cheese, and instant potato mash represented on the window of dimensional stability below the 5% deformation-tolerance line would produce dimensionally stable 3D printed structures. Therefore, the screening method provides good practical guidance on determining material printability before the 3D printing process, thus nullifying the need for printing tests of unfit food inks.

Guo, Zhang, and Devahastin (2020a) experimented with the simulation of food grain gels' fluid characteristics during the 3D printing process using computational fluid dynamics. The authors explored the Bird-Carreau model for the simulation and found it to describe better the grain gels' extrusion flow behavior than the rheological test. The researchers reported that the simulated results of the required piston pressure for 3D printing of the gels were consistently verified with those obtained from the real printing test. Thus, they proposed simulated piston pressure as a criterion to evaluate and predict the gel's printability.

Novel alternative, quick, and nondestructive analytical assays such as low field nuclear magnetic resonance (LF-NMR) and near-infrared (NIR) spectroscopic parameters have also been proposed to predict the rheological characteristics of mashed potatoes and potato pastes, indirectly, thus were helpful for further prediction of their 3D printability (Liu, Zhang, and Ye 2020; Chen, Zhang, Guo, et al. 2021). The concepts were based on their known applications to determine the mobility of food composition. Hence, the binding extent of water molecules with macromolecules strongly relates to food material rheological properties. Chen, Zhang, Guo, et al. (2021) employed predictive models describing the relationships between rheological parameters/properties and NIR spectroscopic parameters, revealing reasonable prediction of change in the G' by partial least square, G* and G" by a back propagation-artificial neural network and consistency index by principal component regression. These approaches eliminated the need for time-consuming printing and rheological tests to determine similar food material printing behavior.

3.1.4. Material physical characteristics

The particle size distribution of the food matrix is a critical factor to changes in ink rheological properties, with consequent effects on food printability (Feng et al. 2021). The researchers evaluated the particle size distribution ($929.77 - 471.17\,\mu m$) effect on rheological properties and printing characteristics of carrot pulp gel. The preferred higher apparent viscosity of the inks containing smaller particle sizes (545.05 and $471.17\,\mu m$) was attributed to the higher expression of more macromolecules linked with water through hydrogen bonding/intermolecular forces. A possible larger surface area with decreasing particle size might have also resulted in increased G', G", printing stability, gumminess, cohesiveness, and less than one tan δ value. In turn, both 3D printed gels were characterized with higher 3D printing performance, more uniform pore size distribution, and better order of microstructures (Feng et al. 2021).

Lee et al. (2019) used a different ink system (dispersed ink containing spinach powder (SP) and xanthan gum), lesser particle size distribution ($50 - 307\,\mu m$), and evaluated similar properties. They observed an increasing SP particle size improved the ink system's hydrodynamic stability due to the formulations' high-volume fraction. Their observation was also evident with increases in G', G", and shear modulus which were in proportion to rising particle sizes. Although the inks' mechanical strength differs, all formulations were reported to be printed smoothly irrespective of the particle sizes examined.

Despite using distinct ink systems, both studies' findings suggest the best printability by modifying particle-particle surface contact to induce appropriate consistency between fluidity and adequate mechanical strength of ink to produce better ink printing performance and structures with good shape-retention.

3.1.5. Use of modifying agents and pretreatment techniques

It is germane to note that the inclusion of modifying agents and pretreatment techniques may alter the morphological state and presence of participating constituents in prepared food ink. Such intra-/inter-molecular interactions could influence rheological properties' changes and cause potential variations in material printability (Dankar et al. 2020). Dankar et al. (2020) examined the effect of microwave heating (700 W for 6 min) and boiling (at 98 ± °C for 20 min) of potato and then the inclusion of varying additives on the rheological and mechanical properties of prepared food inks. Compared with boiled samples, microwave heated potato purees showed more aggregated and densely concentrated starch granules that supported up to five times a significant increase in the thixotropic areas (stronger internal stability), viscosity, yield stress (internal elasticity), cohesiveness, consistency, and firmness. The inclusion of 1% butter to microwaved sample enhanced lipid-starch complexes' formation, which influenced creamy surface texture and best printability in terms of continuous smooth extrusion and higher self-supportability (Dankar et al. 2020). Xu, Zhang, et al. (2020) studied the impact of heat treatment conditions (temperature and time) on egg yolk printing characteristics with no additives. At 76 °C for 8 min, the resultant egg yolk pastes exhibited shear-thinning behavior and solid-like gel indicating that G' values were greater than or equal to G". The printable viscous gel properties were related to the extent of protein denaturation, facilitating the release of free lipids and the gradual formation of the tightly bound protein-water-lipid network.

Using synergistic treatments, Fan et al. (2020) reported positive alteration in dielectric properties of soybean protein isolate and strawberry slurry ink using low power [30, 50, and 70 Wattage (W)] microwave synergistic salt pretreatment for 4 minutes (min). The highest microwave absorption performance of the treated ink system (salt-70 W, to attain 71.60 °C core temperature) resulted in the best 3D structure accuracy, improved formability (increased apparent viscosity and G') and shape stability of printed constructs, least transverse relaxation time (reduced mobility of bound and immobilized water), the optimum value for cohesiveness, gumminess, hardness, springiness, and better volatilization of flavor. Likewise, Guo, Zhang, and Devahastin (2021) experimented with the synergistic addition of calcium chloride (Ca^{2+}) and microwave (MW) heating (700 W to attain 90 °C central temperature) to determine the 3D printability of buckwheat starch-pectin gels. The prepared gel mixture with lower viscosity was observed due to aggregation brought about by the amide group's cross-linkage with Ca^{2+}, which led to the fraction release of bound moisture to the matrix. The synergistic pretreatment for 30 seconds (s) was suggested to have improved the gel printing precision, and 1% Ca^{2+} inclusion was intuitively judged with the best printing performance compared to other gel mixtures with lesser additions.

Xu, Zhang, et al. (2020) explored a combined pretreatment of ultrasonic- microwave heating effects on the 3D printing quality of wheat starch-papaya paste suspension. The researchers used the same ultrasound treatment (UT) condition and varied microwave power density (60 W, 70 W, and 80 W). The tandem pretreatment of paste suspension by UT and microwave power of 80 W resulted in increases of G', G", and bound water ratio. Decreases in the properties were recorded for suspensions treated with lesser microwave power density. As the authors inferred, UT increased liquidity in the system with a low degree of gelatinization. At the same time, UT influenced the higher water absorption and swelling capacity of starch granules in a high degree gelatinized system (at 80 W). Thus, the printed structure pretreated with UT and microwave heating at 80 W showed higher printing accuracy and better shape retention.

The above findings revealed standalone pretreatments, or in combination with modifying agents or other pretreatments, could induce discrete printing effects on different non-printable materials. A recent review has suggested that microwaving, combined with other techniques, is better for modifying starch components in food, particularly influencing swelling capacity, pasting property, and gelatinization (Oyeyinka et al. 2021). The suitability of the reported pretreatments was adapted based on nature and material form being experimented with for 3D printing. The pretreatments were generally demonstrated to trigger conformational changes of major biopolymers (including the formation of strong ink network by short-spacing intercellular components), which transform the viscosity and viscoelastic properties of non-printable inks into appropriate fluidity/pseudo-plasticity and sufficient mechanical strength of printable inks, the prerequisite for good printing performance and better shape stability. Along with the desirable and improved printing effects on non-printable material, further study should be designed to mitigate some adverse impacts on other quality properties such as the nutritional components and sensory features.

3.1.6. Food ink storage conditions before printing

It is also vital to stress the effect of resting or storage temperature and time of food ink before 3DFP. These conditions contribute to dynamic changes in viscosity profile and rheological properties of printing inks, most especially starchy material, in terms of the starch source, retrogradation effects, and re-proportion degree of starch polymers (Maniglia et al. 2019; Liu, Tang, Duan, Qin, Zhao, et al. 2020; Paolillo et al. 2021). There is, however, less reported information about the extent of those conditions' influence on food ink printability. Paolillo et al. (2021) investigated the effect of resting times [2, 24, and 46 hours (h)], printing temperature, and varied ingredients of starchy gels stored at room temperature. Increasing storage time at ambient temperature was found to significantly increase the ink gel's viscosity, which was suggested to be due to amylopectin chains' rearrangement, occurring at a lesser rate than amylose gelation. However, 24 h of resting duration, the mixed fraction of maize starch (10 g/100g) and tapioca dextrin (30 g/100g), and printing temperature (45 °C) were found to synergistically modulate higher G', the moderate limit of tan δ, shear-thinning behavior, and best printability of the printed object.

3.2. Printing parameters

As highlighted in Section 2, dual effects of food material properties and printing parameters may determine the success of 3DPF structures. Available studies on 3DPF items summarized in Table 1 indicated that the 3D printing parameters are uniquely tuned to match a specific food ink formulation's printability. Accordingly, determining an optimum link between these two principal factors may bring about consistent printing quality of 3DPF products (Dankar, Haddarah, et al. 2018). The primary printing parameters influencing the final printing quality of printed constructs include nozzle diameter (ND, the diameter of printing nozzle), nozzle movement speed (NMS, the velocity of nozzle movement of extrusion head(s) during printing), printing temperature, and nozzle or layer height (NH or LH, the distance between the extruder's nozzle tip and the printing stage/deposited top layer) (Dankar, Haddarah, et al. 2018; Pérez et al. 2019). Thus, the food matrix undergoing printing is also reformed with respect to the applied printing conditions. Therefore, implications of varying changes on the quality properties of printed food products are expected.

Yang, Zhang, Prakash, et al. (2018) investigated the influence of ND, NH, NMS, and extrusion rate on the printing quality of lemon juice gels. They stated that the printing nozzle diameter directly determines the extruding filament precision and 3D constructs surface roughness. The authors considered equal value for NH and ND to be appropriate for the experimented gel's print quality and attributed occurring defects under this condition to be the mismatched between printing speed and extrusion rate, provided no expansion or shrinking/swelling of the extruded ink. The same NH and ND values could be used to avoid droplet formation, line deformation, or protrusion effects of printing material during 3D printing operations (Fahmy, Becker, and Jekle 2020).

In an experimental study by Yang, Zhang, Fang, et al. (2019), the process optimization of NMS, ND, filament diameter (FD), and NH affected the geometrical accuracy of the 3D printed baking doughs. FD, NMS, and ND's process variable effects were attributed to changes in the doughs' apparent viscosity, which influenced varying printing resolutions during the mechanical shearing printing process. Diañez et al. (2019) stated that both printing speed and LH are related to the printing ink flow; the former may determine the required residence time of printed ink on bed/previous layer to be properly self-structured, while the LH is linked to the volume of deposited ink that needs to be self-structured. Yang, Zhang, Fang, et al. (2019) recommended NH best modeling effect of printing dough to be close to FD, considering the need for uniform fuzing of printed layers to achieve a desired extruded geometry accuracy. A 75% LH setting of the nozzle diameter was found to maintain printed paste shape containing fiber and protein-rich components (Krishnaraj et al. 2019). Therefore, these findings suggest that equal NH and ND settings may not be the optimum printing conditions for all food inks to obtain a product with precise and accurate structural dimensions. Thus, the significant printing effect by LH and ND may determine the bonding ability of successive layers, structural stability, and overall printing fidelity of an edible construct (Dankar, Pujolá, et al. 2018; Krishnaraj et al. 2019).

The simultaneous printing effects by NMS and extrusion rate (both control the amount of extrusion per unit length per unit time) were found to be positively correlated (Yang, Zhang, Prakash, et al. 2018). Increased printing speed intensity may cause dragging of the deposited filaments with an outcome of breaking lines of extrusion. On the other side, low printing speeds could result in flow inconsistency and build-up of unsolidified printed layers with poor stability (Liu, Meng, et al. 2019). Similarly, a low extrusion rate may result in discontinuous extruding filament lines, while the higher rate could lead to filament overlap and significant deviation to the targeted CAD (Yang, Zhang, Prakash, et al. 2018). Derossi, Paolillo, et al. (2020) examined the screw-based deposition system at medium-high speed, and the effect of non-printing movements/variables on the final quality of 3D printed cereal-based constructs. They reported two different options to improve the print speed beyond the limit of 70 mm/s, either using a flow of 300% or setting FD at 1.0 mm. They recorded oozing and stringing defects due to the nozzle's retraction distance, which was more relevant to printing quality. In contrast, retraction speed and travel speed were vital to minimize printing time. Further experimental probing of the undervalued printing parameters at 200 mm/s print speed, 100% flow, and 1.0 mm filament diameter gave a good replica of the virtual models. Hence, an optimum equilibrium between the printing parameters and non-printing variables is necessary for achieving uniform extruding FD and smooth line of extrusion to replicate precise layers of a virtual model.

Liu, Tang, Duan, Qin, Zhao, et al. (2020) investigated the effect of different NDs and printing temperatures on the viability of probiotics (*Bifidobacterium animalis* subsp. Lactis BB-12) in 3D printed mashed potatoes. The authors revealed that the least nozzle diameter (0.6 mm) caused a significant reduction of the probiotic viability (9.93 − 9.74 log CFU/g) due to the nozzle shear stress intensity. Considering that food ink will be maintained in the extrusion barrel while printing progresses, they also determined the effect of holding time (15, 25, 35, and 45 min) of mashed potatoes at varying printing temperatures (25, 35, 45, and 55 °C). The highest reduction of probiotic BB-12 strains viability (9.26 − 7.99 log CFU/g) was observed at the maximum printing temperature of 55 °C and holding time of 35 − 45 min. Although the temperature range experimented was less significant on mashed potatoes' printability, its probable effects on printing behavior of other inks (such as chocolate) and the need to retain a substantial level of bioactive components in temperature-controlled 3D extruded products position its vital consideration in 3D food printing applications.

Few studies have experimented with the influence of printing parameters on the composition of printed food products. One of such examined the effect of different print speed and percentage flow on fruit and vegetable-based ink properties (Severini, Derossi, et al., 2018). The researchers reported less influence of the parameters on the printed smoothie's health-promoting properties (antioxidant capacity and total phenolic content). However, the printing temperature was not provided. There was also no significant modification in the samples' sensorial characteristics (Severini, Derossi, et al., 2018). Future experimental studies should investigate the nutritional, health-promoting, physicochemical, and in-depth sensory qualities of printed structures to properly understand the effects of printing parameters after post-deposition. Nonetheless, the digitalized deposition of food matrices to form complex structures may determine compositional quality retainment in proportion to the degree of printing condition (i.e., temperature) or exposure to post-processing treatments (Diaz et al. 2018).

3.3. Pre- and post-printing treatments

Printable food inks are generally pre-processed, which may be sufficient for desired palatability after printing operation, or semi pre-processed, requiring post-deposition treatments to ensure edibility. The majority of available 3DPFs are mostly printed at room/ambient temperature (Table 1). Printed foods like mashed potatoes, chocolates, cheese, smoothies, breakfast spread structures are suitable for direct consumption. Others in paste, slurry or dough-like printed products require post-deposition processing prior to consumption (Table 1).

The choice of printed food post-processing techniques could depend on a suitable cooking mode, which elicits unique gustatory and other sensory features with good acceptability. For instance, microwave heating may find better cooking applications to drive out moisture and retain compactness and dimension of printed structures compared to boiling (Dankar et al. 2020). The generally adopted post-processing treatments include baking, frying, drying, and steaming (Table 1), with varying effects reported on the printed food product. Pulatsu et al. (2020) reported tapioca cookie dough formulated with reduced sugar content and no added gelling or stabilizing substances. This formulation yielded structurally stable 3D printed structures after baking. Similarly, printed and baked snacks prepared from wheat flour dough containing ground insects resulted in the modification of the main microstructure and dimensional properties (Severini, Azzollini, et al. 2018). Zhang, Lou, and Schutyser et al. (2018) examined probiotics' survival in 3D printed wheat dough structures with different surface-to-volume ratios during baking. Their result showed that the printed structure's geometry was well preserved during baking, and the baking process of the construct with the highest surface-to-volume ratio was enhanced. The latter product baked at 145 °C for 6 min met the recommended range of viability for probiotic foods. The fast-cooling process of low-gluten flour dough at −65 °C for > 10 min after 3D printing was useful to maintain the printed product's shape and structure stability after the further baking process (Yang, Zhang, Fang, et al. 2019). The effect of baking and steaming treatments on printed egg fraction was reported to have significantly impacted the retention of shape of the treated structures (Anukiruthika, Moses, and Anandharamakrishnan 2019).

Steamed 3D printed doughs prepared from rice varieties were examined by Liu, Tang, Duan, Qin, Zhao, et al. (2020). Rice dough containing high amylopectin content resulted in structurally stable printed constructs. Still, it was observed to have swollen during steaming and gave the worse shape stability and highest starch hydrolysis rate. On the other hand, after printing and steaming operations, rice types comprising high amylose contents showed better printing performances and structural stabilities and increased resistant starches. In this study, the swelling and hydrolysis rate was suppressed due to amylose-lipid complexes' formation. The high percentage of the retained starch fraction was associated with less susceptibility to enzymatic attack (Liu, Tang, Duan, Qin, Zhao, et al. 2020).

The printed samples of protein-based pastes with high initial solids content (<50%) were better adapted for oven drying than freeze-drying treatment (Lille et al. 2018). According to Krishnaraj et al. (2019), the microwave drying of 3D printed snacks containing barnyard millet, fried gram, green gram, and ajwain seeds could better preserve nutrients with slight changes in textural and color properties.

Feng et al. (2020) prepared composites of yam powder and potato processing by-product powder and examined the 3D printing characteristics of the air-fried structures. They reported that infill structures influenced the degree of bending height of the post-processed product with respect to the direction of the printed filament line, which is exposed to the treatment, thereby possibly changing form due to the direction of water loss and shrinkage. Infill parallel structure resulted in minimal bending height of the air-fried snacks. Infill levels were observed to have affected the porosity and weight of the 3D printed products. Similarly, 3D printed and air-fried potato-based snacks were reported to show slight shrinkage after the post-printing treatment (Liu, Dick, et al. 2020). Based on the printed food material examined, different post-printing treatments could affect or improve the quality of the 3D printed product. Several factors such as the mechanism for cooking effect, availability, cost, and preference could influence the choice of these post-processing treatments. They would thus need to be considered for the printability of fermented or malted food materials.

4. The current state of research on 3D printed foods and applicability for fermented and malted foods

Available studies on 3DFPs have shown the significant application of 3D printing technology for a diverse range of materials, including cereals, root, and tubers, fruit and vegetables, confectionery, egg and egg products, fish and fish products, legumes as well as milk and milk products (Table 1). Others include products made from hydrocolloids/

hydrogels and starches. The current trend in 3DFP is to make available more customized and attractive food designs based on digitalized nutrition to meet specific healthy lifestyle requirements. The 3D printing technology has been employed to integrate bioactive molecules, probiotics, nutrient-rich substrate, or functional ingredients in complex food matrix containing food additives (including natural gelling or thickening agents). These attempts may enhance the mastication process, support shape fidelity, and resist the printed product's deformation. Surprisingly, there are probably no available studies in the literature reporting on the 3D printing of fermented and malted food products. Our initial search on Food Science and Technology Abstracts database using "*3D printing* and *food*" as keywords resulted in 155 studies and Web of Science, 289 results. A slight modification of this search item to include either *ferment*, *fermentation*, *malt*, *malting,* or *malted* yielded no meaningful, applicable result and, in some instances, no results. The only exception was a study by Rodgers (2016) when "*3D printing and food and ferment/fermentation*" was used for the search. A further probe of the article (Rodgers 2016) indicated that 3DFP was highlighted as a potential novel technology for value addition to minimally processed functional foods, including fermented foods in that study. Nonetheless, a review of available literature indicates that some substrates have been utilized for 3D printed foods, most of which are already summarized in Table 1.

Several studies on the major and optimal printable formulation and printing parameters for 3DFPs could provide an empirical baseline for developing and further investigating other food types, such as those obtained through fermentation and malting. While few were 3D printed at elevated temperatures (55–85 °C), leading to products that may be ready for consumption, most were 3D printed through CE (at room temperature). The resultant 3D structures for the latter were thus subjected to varying post-processing techniques to obtain edible products. The reported optimal printing parameters differ significantly with variation in the food matrix and the configuration of the 3D printer employed in the printing process and associated software. In most cases, slight processing/pretreatment of food ink (e.g., melted chocolate) or ingredient formulation containing natural additive, gelling, or thickening agents has engineered the printability of the 3DPFs. The added quantity of food-grade hydrocolloids/hydrogels is often low and enough to optimally regulate the desired rheological and mechanical indices of food ink formulation for printability (Portanguen et al. 2019). Although food-grade chemical additives are frequently used, there is a gradual shift toward additives from natural sources. From the consumer health standpoint, additive blending to realize a printable product may be a significant barrier toward developing large-scale functional foods due to concerns around additives and demand for minimally processed foods. Therefore, the way forward could either be using appropriate pretreatment techniques, optimizing food matrix component without the addition of additives as demonstrated in few studies (Krishnaraj et al. 2019; Liu, Tang, Duan, Qin, Zhao, et al. 2020), or incorporation of natural additives that tend to support both proper flow behavior and function as nutritional aids (Table 2). Little quantities of pigments like sunset yellow and anthocyanin are also added to improve the resulting printed structures' appearance (Liu, Dick, et al. 2020; Liu, Tang, Duan, Qin, Zhao, et al. 2020). Using these measures, the pictorial views of the developed products presented in Table 2 are promising, with good printing resolution and structural stabilities. These concerted efforts encourage more of such edible 3D constructs tailored for improving wellness.

Azam, Zhang, Bhandari, et al. (2018) demonstrated successful 3D printing of fruit-based construct by incorporating Vitamin D in orange concentrate and modified the food system with κ-carrageenan gum and wheat starch. Likewise, selected fruit and vegetable blends have been 3D printed into shaped snacks (Derossi et al. 2018; Severini, Derossi, et al., 2018; Pant et al. 2021). Protein-based structure chiefly containing semi-skimmed milk powder and other ingredients prepared as paste presented the best construct among other food materials experimented (Lille et al. 2018). Similarly, a milk protein paste mainly consisting of milk protein concentrate and whey protein isolate gave a close replica match to the virtual designed model (Liu, Ho, et al. 2018). As a novel protein source, wheat flour dough enriched with different quantities of yellow mealworm powder was 3D printed into snacks with sufficient structural fidelity (Severini, Azzollini, et al. 2018). Ghazal, Zhang, and Liu (2019) made 3D printing of a healthy food mix of anthocyanin, potato starch, and lemon juice gel with attractive colors. Composite flour rich in fiber and protein from indigenous ingredients (barnyard millet, fried gram, green gram, and ajwain seeds) were formulated, and 3D printed as snacks with the best resolution and stability at optimized printing parameters (Krishnaraj et al. 2019). In the same vein, printed snacks containing yam and fiber-rich potato processing by-products have been demonstrated to display good printing characteristics with similar structures to the model geometry (Feng et al. 2020).

Enriched, printed, and baked snacks with ground insects were reported with a corresponding significant increase in the total essential amino acid, protein digestibility, and corrected amino acid score (Severini, Azzollini, et al. 2018). Edible insects as novel and affordable sources of proteins in food have been reported and are known to contain appreciable bio-components with nutritional and therapeutic properties (Cho et al. 2018; Cho et al. 2019; Kewuyemi, Kesa, et al. 2020). In light of the above reported studies on the printed food structures suggested being rich in health-promoting components could, therefore, be potentially appreciated or improved through the bio-modification processes of fermentation or malting techniques (Adebo 2020; Ohanenye et al. 2020).

The particular interest in fermented and malted products is related to these traditional processes' simplicity and their beneficial modifications and improvement they confer to foods. Both processing techniques are known for the desirable attributes they confer to foods, including pleasant aroma, texture, color, and other sensorial properties, as well as appreciable modification in nutritional components and health-promoting properties (Adebiyi et al. 2017; Taylor and Taylor 2017; Adebo and Medina-Meza 2020). Others include reduction of antinutritional factors, improved nutrient digestibility, enhanced physical and technological characteristics, and extended food shelf life (Figure 4). These beneficial effects differ in the processed substrate and process conditions employed, which are usually made possible by microbial metabolism stimulating rapid degradation or formation of bio-components during fermentation or malting (Verni, Verardo, and Rizzello 2019; Ohanenye et al. 2020; Kewuyemi, Njobeh, et al. 2020; Chinma et al. 2021). As earlier highlighted, the fermentation process may be initiated by natural microbiota (natural or spontaneous fermentation) or inoculation of suitable microbial strains (controlled fermentation). Dallagnol et al. (2013) investigated the controlled fermentation of quinoa sourdough by *Lactobacillus plantarum* CRL 778 and revealed the significant concentration of free amino acids, peptides, and phenyllactic and hydroxyphenyllactic acids (antifungal compounds). Rizzello et al. (2015) inoculated *L. brevis* AM7 and *L. plantarum* C48 in flours from legume varieties to prepare sourdoughs. They reported fermented sourdoughs influenced the number and intensity increase of lunasin-like polypeptides. Also, the extract of few sourdoughs decreased the proliferation of human adenocarcinoma Caco-2 cells viability up to 70%. The experimental work of Gabriele et al. (2019) showed that sourdough fermentation of bean flours significantly increased ascorbic acid, flavonols, total polyphenols, and reduced phytic acid content. The antioxidant activities of the fermented product demonstrated a strong inhibitory effect on low-density lipoproteins oxidation.

Aguilar et al. (2019) reported that malted quinoa grains showed increased protein content, ascorbic acid, flavonoids, phenolic compounds, reducing sugars, and antioxidant capacity. Consistently, Nelson et al. (2016) revealed that malted whole-grain (WG) wheat had significantly higher antioxidant activity and polyphenol content than the non-malted WG wheat. These researchers also measured obesity-related biomarkers, including diastolic blood pressure and low-density lipoprotein. They reported that the former reduced significantly with time, while the latter increased slightly over time with the breakfast cereals as a dietary intervention. The insulin resistance also increased with malted wheat (Nelson et al. 2016). Germination, a critical process in malting, was demonstrated by Luo et al. (2014) to influence the varying availability of calcium, copper, iron, manganese, and zinc in germinated faba bean, rice, soybean, and wheat grains. Comparably, copper, sodium, and zinc increased in sprouted *Chenopodium album* flour (Jan, Saxena, and Singh 2018). Additional increase in dietary fiber, fatty acids, protein, and viscoelastic property (storage modulus) of the flour was also noted. Setia et al. (2019) demonstrated enhanced pasting viscosities of germinated faba bean and yellow pea flours at ambient temperature for 24 h. They observed improved foam stability, foaming capacity, emulsion activity and stability, and the *in vitro* digestibility of the flours' protein and starch. Theodoro et al. (2021) carried out an *in vivo* study using germinated millet flour as a dietary intervention. The flour's functional biological effects were reported to show antioxidant activity, increased anti-inflammatory cytokine, and reductions in inflammatory markers, adiposity, and liver steatosis. Considering the above, the nutraceutical potentials of fermentation and malting combined with 3DFP can yield novel and value-added 3D food structures for better well-being.

Although there is no available study on fermented or malted 3D printed products, several value-added or ready-to-eat food products have also been developed from these processes using other techniques (Table 3). These include but are not limited to biscuits, bread, cookies, extruded products, and snacks. The innovativeness of 3DFP has been demonstrated to produce attractive novel food structures enriched with probiotic strains. Liu, Tang, Duan, Qin, Zhao, et al. (2020) demonstrated the inclusion of *Bifidobacterium animalis* subsp. Lactis BB-12 in 3D printed mashed potatoes and observed higher bacteria viability (>7.99 log CFU/g) than the specified level in probiotic-containing foods. Similarly, Zhang, Lou, and Schutyser (2018) incorporated probiotic bacteria (*Lactobacillus plantarum* WCFS1) into a 3D printed wheat dough. They reported that a higher surface-to-volume ratio of the printed construct supported the survival of the probiotic microorganism. These experimental findings demonstrated a promising prospect for the integration of functional ingredients in the printed food matrix. In addition, to diversify the available printed functional foods by developing printable fermented or malted food products that could meet consumer needs. This applicability could target better delivery of functional foods with novel and unique geometry structures containing essential nutrients and health-improving components. More importantly, detailed screening of potential traditionally processed-3D printed foods at the molecular level using omics approaches would provide interesting data to validate their rational promotion as attractive superfoods with distinct wellness values (Adebo et al. 2021; Theodoridis et al., 2021).

5. Advantages and limitations in food product development with 3D printing

In 2009, Cohen and other researchers presented the major barriers in 3D food printing applications (Cohen et al. 2009). The then highlighted and still trending constraints in developing 3D fabricated foods include suitability of materials for printing, high cost of 3D printer, lack of food-based printing firmware and software applications, and less incorporation of food-safe printing components (e.g., steel syringes). Despite the drawbacks, as evident in recent studies, researchers have intensified efforts to develop a significant range of 3D printed foods using several modification approaches and transformation of open-source printing platforms for food applications (Table 1). The group of successfully 3D printed edibles would continue to expand the market shares for more innovative printed meals. The processing limitations, advantages, and suggestions for future

Table 2. Reported pre/post-processed 3DPFs with natural additives or no gums/stabilizers.

3D printed food structures	Natural additive and quantity used	Function of natural additives	Virtual 3D model used	Pictorial view of optimized pre- and post-processed products	References
Air-fried yam snacks	Pectin (17%)	NS	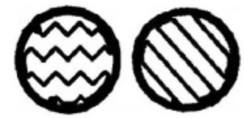		Feng et al. (2020)
Baked wheat snack	NA	NA	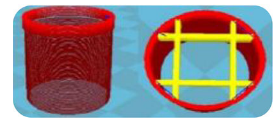		Severini, Derossi, and Azzollini (2016)
Baked wheat and mealworm snack	NA	NA		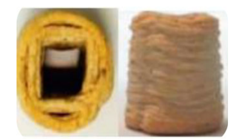	Severini, Azzollini, et al. (2018)
Baked wheat-based structure containing probiotic bacteria	Calcium casienate powder (3%)	Largely improved dough printability			Zhang, Lou, and Schutyser (2018)
Dark chocolate	Plant sterol powder (3%)	Improved the flow of chocolate	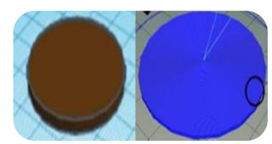		Mantihal, Prakash, and Bhandari (2019)
Fruit-based snack	Pectin solution (11%)	For sufficient consistency and avoid phase separation	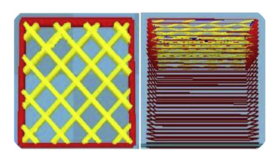	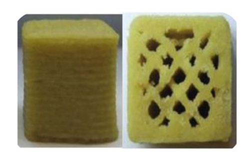	Derossi et al. (2018)
Heat-induced egg yolk paste	NA	NA	NP		Xu, Zhang, et al. (2020)

Mashed potato	Citric acid (1%)	Increased apparent viscosity, storage modulus, gumminess, and hardness	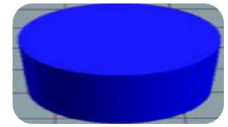		He, Zhang, and Guo (2020)
Microwaved fiber-rich snack	NA	NA	NP		Krishnaraj et al. (2019)
Smoothie	Fish collagen (1%)	To slightly increase the paste viscosity	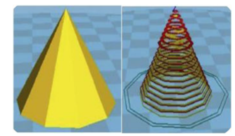		Derossi et al. (2018)
Steamed rice product	NA	NA	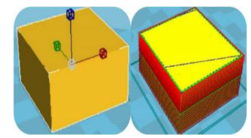		Liu, Bhandari, et al. (2020)

NA, not applicable; NP, not presented; NS, not specified.

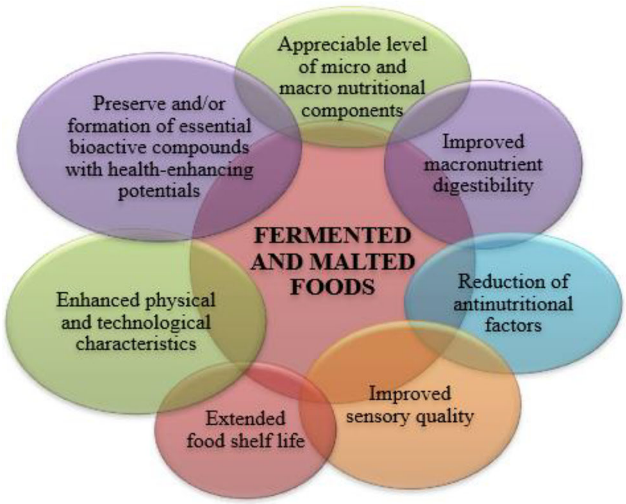

Figure 4. Benefits of fermentation and malting.

investigations are further discussed in the following sub-sections.

5.1. Available firmware and slicing software

Several 3D printers with a built-in firmware and available slicing software are used to communicate the detailed mechanical path of a model for precise deposition of materials into layers. The commonly used slicing software packages for disseminating planned mechanical route instructions and processing conditions to 3D printers are programmed explicitly for printing thermoplastic polymers. These include Cura, Repetier-Host, Rhinoceros/Rhino 3D, Slic3r, and Slimplify3D (Table 1). The composition of the thermoplastic material and behavior during printing greatly differ from edible inks. The existing slicing packages have been programmed so that certain key parameters like nozzle size (mm) are used to estimate dependent parameters such as infill line width, number of outside wall lines, and wall thickness. Shell thickness (mm) combined with nozzle size is, for example, used to compute perimeter lines' number and thickness in Ultimaker, Cura 15.04.6 software. Similarly, extrusion rate is determined by extrusion multiplier, filament diameter, and printing speed inputs in simplify3D software (Fahmy, Becker, and Jekle 2020). The elasticity nature of printing food material with possible expansion may result in some printing inconsistencies during deposition or after food printing operations.

Although, edible printed constructs without adverse slicing effects on their structural characteristics have been demonstrated. Severini, Azzollini, et al. (2018) reported a nearly doubled percentage volume fraction of a digital model solid phase (30 g/100g) from an initial of 36% to about 69% in wheat substituted with edible insect printed snacks. In comparison with the fitted nozzle size (0.84 mm), similar mismatches were noted for the deposited filaments (1.5–2.7 mm) and conjunction zones (3.0–4.3 mm) thicknesses at different ink formulations (Severini, Azzollini, et al. 2018). Liu, Meng, et al. (2019) also reported larger wall thicknesses of multi-component gel models' deviations from the CAD model. Thus, considering the significant disparity between food materials and plastics, it is necessary to optimize available slicing software for food printing operations or a much better and lasting solution of developing slicing application packages for manufacturing 3D printed foods (Guo, Zhang, and Bhandari 2019a). Such developed applications suited for food printing will immensely facilitate the use of 3D food printers, especially on an industrial scale where consistency in products' geometry is necessary.

5.2. Choice of 3D extrusion printers and cost implication

The proprietary restrictions, prohibitive cost, and inflexibility of the component-part of printing systems were limiting factors for the growth of 3D food printing applications (Cohen et al. 2009). However, the advent of RepRap (replicating rapid prototype) open-source 3D printing machines, e.g., the Prusa i3 3D printer (Prusa Research, Prague, Czech Republic), has substantially surmounted these challenges. Most of such commercially available printers used are either Cartesians or Delta configurations, and the price ranged from 160.00 to 6,650.00 US dollars (Carolo 2020; 3dsourced, 2021). Such consumer-styled printing platforms have been successfully transformed (i.e., by incorporating syringe-based deposition systems) for food printing applications (Table 1).

More recently, there are now available and dedicated edible desktop 3D printers such as the Foodbot 3D Food printers (China), Natural Machines Foodini (Spain), byFlow Focus 3D food printer (the Netherlands), among others, with application supports (byFlow 2021; FoodBot 3D 2021; Natural Machines 2021), albeit still expensive (300 – 4,659.91 US dollars) (Lansard 2021). The online or offline supports (e.g., byFlow Studio and Foodini Creator software) offer 3D food design collections, food recipes, tools for designing personalized models, etc. The recommended 3D food printing applications include biscuits, chocolate, cake, cheese, creamy candy, meat, mashed potato, paste, puree, and jam. The printers are custom-built with simple control digital interface and satisfying food hygiene specifications such as enclosed printing platforms, less contact with printer parts, stainless steel cartridges/barrels, food-grade plastic parts, food-grade silicone mat, and are generally easy to clean.

Furthermore, future modification of FDM desktop printing platforms using food-grade components would still find substantial application for 3D printing of substrate with greater mechanical strength. More experimental studies by the culinary community using digital extrusion-cooking machines for a vast range of raw materials would channel more innovative 3D printed products for individualized consumers and new opportunities, including the best design of industrial-sized 3D food printers for large-scale commercialization.

5.3. Design of extrusion mechanism

As previously mentioned in Section 2, the 3D food printing extrusion mechanisms are based on screw (driven by stepper

Table 3. Value-added ready to eat food products from fermentation and malting.

Raw material	Post processing	Final product	References
Fermentation			
African yam bean	Baking	Bread	Chinma et al. (2020)
Chickpea blend	Extrusion	Extrudates	Yağci et al. (2020)
Goat meat and soy protein concentrate	Cooking	Cabrito snack sticks	Cosenza et al. (2003)
Maize flour	Frying	*Kokoro*	Oranusi and Dahunsi (2015)
Millet flour	Baking	Biscuits	Adebiyi et al. (2017)
Quinoa-based, date, bilberry, and banana	N/A	Gruel	Väkeväinen et al. (2020)
Fermented millet paste	Boiling	Thin porridge	Ojijo and Shimoni (2004)
Fermented rice flour	Extrusion	Noodles	Zhu, Chen, et al. (2019)
Gluten-free sourdough	Baking	Gluten-free bread	Olojede, Sanni, and Banwo (2020)
Legumes and cow's milk	Baking	*Gergoush*	Thorsen et al. (2011)
Chestnut	Drying	Natto-chestnut	Dong, An, et al. (2020)
Cereal-milk mixture	Steaming	Kishk	Gadallah and Hassan (2019)
Sourdough and insect (*Alphitobius diaperinus*) powder	Baking	Snacks	Roncolini et al. (2020)
Sourdough	Baking	Bread	Ktenioudaki et al. (2015)
Fermented wheat dough	Steaming	Steamed bread	Yue et al. (2020)
Oat protein concentrate	Cooking	Oat-based gels	Brückner-Gühmann, Banovic, and Drusch (2019)
Potato, amaranth and chia	Refrigeration	Vegan-spread products	Mosso et al. (2020)
Fermented buckwheat flours	Baking	Water biscuits	Zieliński, Szawara-Nowak, and Wronkowska (2020)
Malting			
Lentils	Baking	Crackers	Polat et al. (2020)
Millet flour	Baking	Biscuit	Adebiyi et al. (2017)
Quinoa and amaranth	Dehydration	Purees	Jiménez et al. (2020)
Brown rice flour	Baking	Gluten-free cookies	Bolarinwa, Lim, and Kharidah (2019)
Sorghum flour	Baking	Gluten-free cookies	Garzón et al. (2020)
Sorghum and tiger nut flour blend	Baking	Gluten-free cookies	Akinwale et al. (2020)
Millet flour	Cooking	Porridge	Ocheme and Chinma (2008)
Millet, sesame, and soybean composite flour	Cooking	Porridge	Alowo, Muggaga, and Ongeng (2018)
Barley and millet flour	Extrusion	Weaning mix	Balasubramanian, Kaur, and Singh (2014)
Millet flour	Extrusion	Instant beverage powder	Obilana et al. (2018)
Chenopodium (*Chenopodium album*) flour	Extrusion	Gluten-free extrudate	Jan, Saxena, and Singh (2017)

N/A, not applicable.

motor) or syringe-driven (air pressure or steeper motor) systems. The study of Liu, Tang, Duan, Qin, Zhao, et al. (2020) depicted a syringe's fusion containing a piston, tightly fitted with a hose supplying compressed air to drive loaded feed in a plastic barrel. This set-up in the form of food-grade steel syringes could be a successful manipulation approach for 3D printing of MFFs in a food-safe manner.

According to Guo, Zhang, and Bhandari (2019b), their simulation investigation revealed that a syringe-based 3D printing system exhibited a simple fluid characteristic with a desirable high shear rate and low pressure at the nozzle outlet. On the contrary, in the screw-based 3D printing system defined with complex fluid characteristics, high shear rate and backflows were observed at the gap between barrel walls and screw flight. Further experimental findings demonstrated that the syringe-based printing system was more appropriate for high viscous mashed potato (potato flakes: water; 1:3) than the screw-based printing system (at 1:6). Notwithstanding, successful screw-based 3D extrusion printings have been achieved with food formulations (chocolates, doughs, gels, and mashed potatoes) containing varying food additives (including gelling/thickening agents) serving as processing or nutritional aids (Table 1). Thus, future screw-based 3D extrusion unit designs could be tailored toward specific food groups for printing precision and shape stability.

While the screw-based system could be preferable for additional printing features like multi-phase food inks printing, plunger/piston programmed with a stepper motor or air pressure-driven syringe/barrel-based system are more efficient for all food ink printings (Table 1). However, the latter mechanisms are restricted to batch printing, and the fitted piston requires more power to be supplied by the programmed stepper motor. In contrast, the former requires lesser operating power, eliminates possible inclusion of air bubbles, improves the homogeneity of printing mix, and is sufficient for continuous feed printing aided by the system's inlet hopper (Guo, Zhang, and Bhandari 2019b).

Moreover, the available extrusion printing systems could be improved by upgrading from the current batch-printing cycles to building remote food-grade stainless steel containers or holding tanks (Lanaro et al. 2017) that are regulated over a range of conditions (i.e., temperature, relative humidity, etc.) for suitability of varying food systems.

5.4. Printing time

The printing time of 3D food printed structures is often not reported in most research studies, making it difficult to ascertain the reported printed constructs' actual processing time. Derossi et al. (2018) 3D printed fruit-based snacks for less than 5 min and Nijdam, Agarwal, et al. (2021) 3D printed different food formulations (e.g., dough, paste, gel, etc.) for 27 to 81 min. Dough-like structures with higher apparent viscosity, G' and G* may require more mechanical force to drive through an extrusion barrel than substrate like gel, chocolate, dispersed ink suspensions, etc. Indeed, the higher ratio of a starchy component in a starchy gel increased its viscosity which necessitated higher dispensing force for 3D extrusion (Paolillo et al. 2021). Therefore, considering that a food ink's required dispensing force is strongly linked to its viscosity, it is reasonable to assume that a constant interplay between timely ink flow under extrusion and higher printing speeds would produce printed structures of preferred lesser energy consumption and reduced processing time.

Further down the extrusion printing channel, the nozzle diameter is a vital determinant for predicting the maximum printing time of a self-sufficient printed construct (Yang, Zhang, Prakash, et al. 2018; Liu, Tang, Duan, Qin, Zhao, et al. 2020). The actual and predicted printing times by common slicing and firmware packages may not match due to unique food behavior during 3D extrusion (Severini, Derossi, et al., 2018). Yang, Zhang, Fang, et al. (2019) observed that different combinations of printing parameters (NH, NMS, FD, and ND) led to varying predicted printing times by the Repetier slicing software. Guo, Zhang, and Bhandari (2019a) stated that layer height controls the height of layers or slices making up a CAD. It is related to nozzle diameter since the diameter is the same as just extruded food filament diameter. Hence, a designed model sliced using a thinner layer height diameter would increase the number of slices/layers with respect to the nozzle diameter under consideration. As such, using a smaller nozzle diameter may imply more detailed slices that will require longer printing time for better precision (Guo, Zhang, and Bhandari 2019a), or the total slices could be suppressed by a higher nozzle diameter, suggesting lesser printing time with a probable adverse effect on printing accuracy and resolution.

Yang, Zhang, Prakash, et al. (2018) experiment further confirmed that to print the same lemon juice gel formulation using a CAD (20 mm x 15 mm), the lesser the nozzle diameter or size used (1.5 mm, 1.0 mm, and 0.5 mm), the higher the required printing time (> 100 s, >200 s, and >800 s, respectively) to complete a 3D structure's extrusion with varying printing resolution. In another study, mashed potatoes printed as cylinder (30 mm diameter and 10 mm height) structures using 1.4 mm nozzle took 273 s and significantly increased to 1304 s when 0.6 mm nozzle was fitted (Liu, Tang, Duan, Qin, Zhao, et al. 2020). Thus, a larger nozzle diameter can significantly lower product printing time by reducing pressure distribution in the flow channel during printing (Yang, Zhang, Fang, et al. 2019). However, the construct precision and total resolution may be adversely affected. Liu, Tang, Duan, Qin, Zhao, et al. (2020) also reported similar increases of the ink extrusion rate through the nozzles; at 0.6 mm = 0.35 g/min and at 1.4 mm = 1.67 g/min. This deviation may partly explain the significant impact of nozzle geometry on the flow stress of food paste relative to the extrusion force (Zhu, Stieger, et al. 2019). Moreover, a logical decision based on the application context would determine a construct selection by considering the print quality and extrusion efficiency.

As discussed above, food printing time could depend on several factors, including the slicing effects by related printing parameter and broadly, the type of printing ink, the capacity of food driving force (i.e., pneumatic or stepper motor), substrate flow behavior and rheological properties, settling time of ink to regain stability during printing, printing performance and characteristics, etc. Because most food inks are paste-like, adequate optimization of the printing parameters is needed, including sufficient resident time on printing beds to ensure an effectively printed material that reduces printing cost for optimum manufacturing efficiency.

5.5. Marketing of 3D printed foods

3DFP technology is an attractive system of food preparation and customization engineered in defined layers. Accordingly, the processing mode exceeds the known barrier of traditional techniques limited to surface designs. The versatility of processing diverse raw materials and growing demand for food products manufactured using this technological prowess are key driving industrial growth to reach an expected global 3DFP market size of 1,015.4 million US dollars in 2027 (Emergen Research 2021).

Food Ink, a 3D-printing pop-up restaurant, emerged as the first of its kind to offer meals prepared using 3D food printers (http://foodink.io/#eclectic). Barilla, an Italian food company, developed the first prototype of a 3D pasta printer to diversify the types of manufactured pasta for consumers' personalized values (Savastano, Amendola, and D'Ascenzo 2018). Its spinout, BluRhapsody, has launched an E-commerce service, where customers can order pre-designed custom pasta or design based on their preference and order customized 3D printed pasta online (https://blurhapsody.com/). The platform is promising for the promotion of a large market share of innovative 3D printed foods. Likewise, is Nourished (https://get-nourished.com/), a UK-based company that "manufactures" personalized foods for health, nutrition, and wellness. They offer pre-packed products and an option to "design" one's food using available options, which can be printed and delivered to homes. This flexibility further demonstrates the potential marketability of 3D printed food products.

The global market size of fermented food and ingredients was forecasted to grow by approximately 55%, from the estimated value of 565.09 billion US dollars in 2019 to 875.21 billion US dollars by 2027 (Emergen Research 2020). The major factors driving the market were highlighted as the increasing need to preserve food produce and the rising perception of fermented product's healthfulness by teeming consumers. Earlier familiarity with sensorial attributes of food products prepared from traditional culinary processes may be crucial to accepting novel traditional food products (Adebiyi et al. 2017; Torrico et al. 2019; Tuorila and Hartmann 2020). For instance, Väkeväinen et al. (2020) study on fermented spoonable vegan products revealed that more than 60 consumers regarded fermented grain-based products as "high in fiber," "healthy," and "novel." Accordingly, adding value to fermented and malted food product through the 3D fabrication of intricate food designs may change dining experience, thus improving the acceptability of 3D printed MFFs. Therefore, prior familiarity with traditional cuisine could play a vital role in the acceptability of printable biomodified substrates. Moreover, 3D printed snacks rich in healthy components have been reportedly acceptable based on sensory attributes (Krishnaraj et al. 2019).

6. Possible scale-up of functional 3D printed foods and future trends

Scale-up strategies are necessary for the continuous advancement of novel innovations such as the 3D food printing technology. The robotic food building process employing dual extrusion 3D food printing aims to give freedom for controlled deposition of printable material(s) composition or distribution within a printed structure (Liu, Zhang, and Yang 2018). The researchers demonstrated multi-extruder printheads to fabricate attractive multi-material constructs containing mashed potatoes and strawberry juice gel with improved geometric complexity and appealing appearance. Likewise, multiple types of chocolate-based inks, consisting of a semi-solid enclosure and liquid filling, were 3D modeled with good self-supporting layers (Karyappa and Hashimoto 2019). Thus, the realization of multi-texture and multi-flavor 3D products is potentially feasible. Such approaches may provide insight for controlled deposition of nutrients and functional ingredients for personalized individual needs in future research studies.

Furthermore, an attractive visual effect of 3D printed functional food products has been realized and found acceptable via an upgrade to four-dimensional (4D) food printing (Chen, Zhang, Guo, et al. 2021; Ghazal et al. 2021). Given this advancement, the potential 3D printing of fermented and malted food products (Figure 5) may position better chances of consumer acceptance and improve with increasing development in the field of food additive manufacturing. Interestingly, our research team has successfully developed fermented and malted 3D printed structures with distinct visual characteristics, no compressed deformation, fewer point defects, and good matching with the targeted virtual model (Figure 6A and 6B). Much more is the possible use of these processing techniques to impact the 4D effect on 3D printed food constructs. These, of course, are promising steps toward promoting a broader range of biomodified printed food products.

Consumer perception is also vital toward the acceptance and possible scale-up of any developed product (Mabotja, Metcalfe, and Adebo 2021), and with food neophobia (fear of trying new foods) (Pliner and Hobden 1992), this might, in part hinder consumers from eating 3D printed foods (Manstan and McSweeney 2020). Metcalf, Wiener, and Saliba (2021) explored the food neophobia scale and the food choice questionnaire to determine food consumers' adoption group's attributes toward a novel food with approved legal status for consumption. The novel product's early consumers were reported to show higher levels of food neophobia, yet greater motivating factors were health, natural content, mood, familiarity, and ethical concern. In a study of consumer perceptions toward 3D printed foods, Manstan and McSweeney (2020) found that out of 329 participants, about 28% believed 3DPF were unacceptable and not safe to consume, although the other 72% were interested in it and eager to try it. In a latter study, similar authors reported observed that the sensory qualities of the 3D printed food were better than the conventional ones, and after consuming the "3D printed" cookie, the participants were willing to eat 3D printed foods and felt they were sustainable (Manstan, Chandler, and McSweeney 2021). Caulier, Doets, and Noort (2020) also reported a similar observation in their study on the acceptance of 3D printed snack bars. While there are indeed potentials for scale-up, appropriate stakeholders will require consumer education to further assist in encouraging the acceptance and consumption of 3D printed foods.

7. Conclusion and future direction

Significant studies have demonstrated extrusion 3D printing for varying food items, including functional ingredients/foods from different raw material classes. Despite the success achieved so far, there is a need to diversify available functional 3D foods and extensively elucidate the nutritional and functional quality thereof. It is also crucial to monitor variations in quality regarding storage conditions and more utilization of natural additives for appropriate modification of material printability. An alternative could be to apply a suitable pretreatment technique to the non-printable material or carefully select food matrix components for better rheological behavior and mechanical characteristics. The optimal match between the key printing parameters relative to the printing substrate's properties is expected to improve 3D food printing efficiency and extrude the targeted geometry's precise filament pattern. During the printing and post-printing processes, the sterilization of each component in contact with food ink at preprinting preparation and overall good processing measures should be ensured to guarantee maximum safety practices and, subsequently, present wholesome products.

Attractive food presentations of 3D printed fermented and malted food products may offer a new consumer experience, promote healthier food choices, encourage healthy nutrition, and strengthen food security. Implementing the above suggestions and developing adequate means to achieve printable fermented and malted food products would be an innovative approach to offer novel 3D foods with improved nutritional and functional properties. Hence, future efforts to widen the available range of printed products to printable fermented or malted foods should systematically modify the process under investigation to the required optimum operating condition. Additional attempts to explore computational and numerical modeling/simulation of the material preparation, fluid flow properties, and process printing variables could facilitate optimum printing conditions prediction for successful food constructs. Concerted efforts by stakeholders in sensitizing the populace about 3D printed foods will still be needed as well as future consideration on developing an effective legal framework/legislation for 3D printed foods to enhance the global acceptance of this innovative technology.

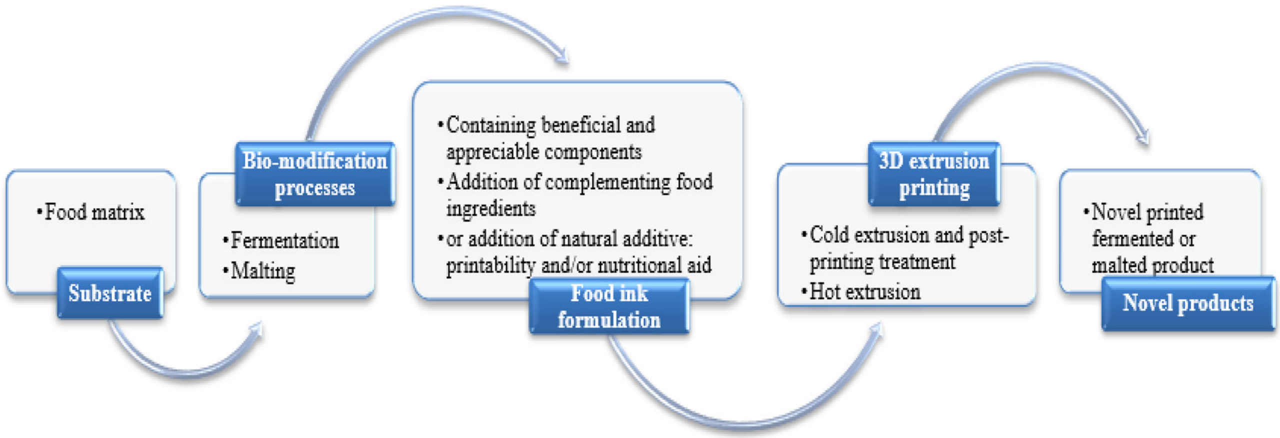

Figure 5. Schematic representation of extrusion-based 3D printing process for the manufacture of novel printable fermented or malted product.

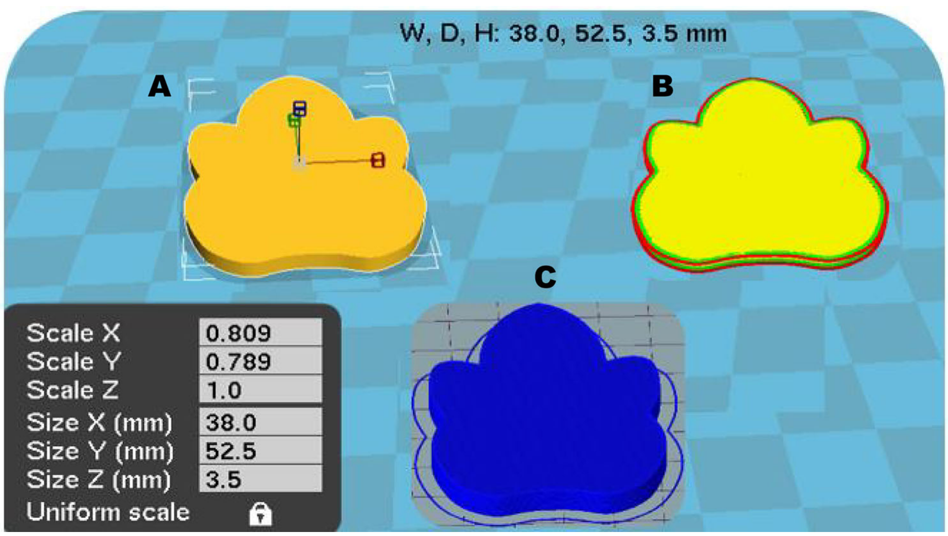

Figure 6A. Virtual 3D models. (A) A model designed using Meshmixer with .stl extension. (B) A model sliced using Cura with .gcode extension. (C) A model detailed printing route.

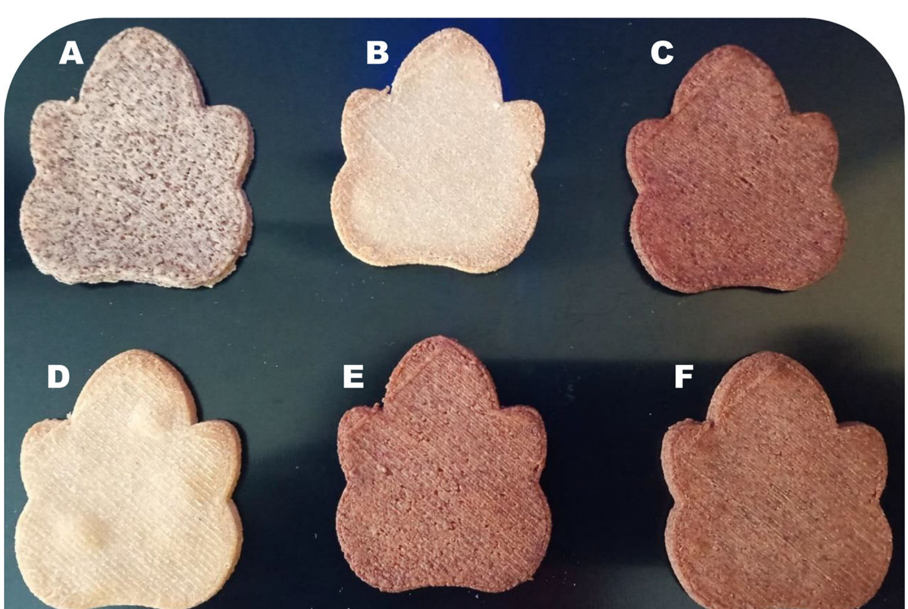

Figure 6B Raw, fermented, and malted 3D printed snacks from our Foodnovate laboratory at the Department of Biotechnology and Food Technology, University of Johannesburg, South Africa. (a) Raw cowpea (b) Raw quinoa (c) 100% cowpea sourdough (CS) (d) 100% malted quinoa (MQ) (e) 80% CS and 20% MQ (f) 60% CS and 40% MQ.

Author contributions

Y. O. Kewuyemi and O. Adebo: reviewed earlier studies, summarized key findings, and prepared the initial draft; H. Kesa and O. A. Adebo: conceptualized the study, supervised, and revised the manuscript. All authors read and agreed to publish the final version of the manuscript.

Conflicts of interest

The authors declare no conflict of interest.

Declaration of interest

A pending patent application (Invention ID: DIS-2021-175) containing the image provided in Figure 6B is being processed.

Funding

This work was supported by the National Research Foundation (NRF) of South Africa DST-NRF Innovation Masters Scholarship (Grant number: 122197); University of Johannesburg Global Excellence and Stature (GES) 4.0 Catalytic Initiative, University Research Committee Grant; and the NRF Thuthuka Grant (Grant number: 121826).

ORCID

Yusuf Olamide Kewuyemi http://orcid.org/0000-0003-3294-245X
Hema Kesa http://orcid.org/0000-0002-1258-9145
Oluwafemi Ayodeji Adebo http://orcid.org/0000-0002-3757-5137

References

7 Best open source 3D printers 2021. 2021. https://www.3dsourced.com/3d-printers/open-source-3d-printer/. Accessed March 20, 2021.

Adebiyi, J., A. Obadina, O. Adebo, and E. Kayitesi. 2017. Comparison of nutritional quality and sensory acceptability of biscuits obtained from native, fermented, and malted pearl millet (*Pennisetum glaucum*) flour. *Food Chemistry* 232:210–7. doi: 10.1016/j.foodchem.2017.04.020.

Adebo, O. 2020. African sorghum-based fermented foods: Past, current and future prospects. *Nutrients* 12 (4):1111. doi: 10.3390/nu12041111.

Adebo, O., and I. Medina-Meza. 2020. Impact of fermentation on the phenolic compounds and antioxidant activity of whole cereal grains: A mini review. *Molecules* 25 (4):927. doi: 10.3390/molecules25040927.

Adebo, O., S. Oyeyinka, J. Adebiyi, X. Feng, J. Wilkin, Y. Kewuyemi, A. Abrahams, and F. Tugizimana. 2021. Application of gas chromatography–mass spectrometry (GC-MS)-based metabolomics for the study of fermented cereal and legume foods: A review. *International Journal of Food Science & Technology* 56 (4):1514–34. doi: 10.1111/ijfs.14794.

Aguilar, J., A. Miano, J. Obregón, J. Soriano-Colchado, and G. Barraza-Jáuregui. 2019. Malting process as an alternative to obtain high nutritional quality quinoa flour. *Journal of Cereal Science* 90:102858. doi: 10.1016/j.jcs.2019.102858.

Ahmed, J., P. Ptaszek, and S. Basu. 2017. Food rheology: Scientific development and importance to food industry. In *Advances in food rheology and its applications*, eds. J. Ahmed, P. Ptaszek, and S. Basu, 1–4. Sawston, UK: Woodhead Publishing. doi: 10.1016/B978-0-08-100431-9.00001-2.

Akinwale, T., O. Ibidapo, S. Owolabi, N. Efuribe, and O. Adeyilola. 2020. Production of gluten-free cookies from blends of malted sorghum (*S. bicolor*) and tiger nut *(Cyperus esculentus*) flour. *American Journal of Food Science and Technology* 8:106–11. doi: 10.12691/ajfst-8-3-4.

Alexander, D. 2020. 3D printing will change the way you eat in 2020 and beyond. https://interestingengineering.com/3d-printing-will-change-the-way-you-eat-in-2020-and-beyond. Accessed March 31, 2020.

Alowo, D., C. Muggaga, and D. Ongeng. 2018. The effect of traditional malting technology practiced by an ethnic community in northern Uganda on in-vitro nutrient bioavailability and consumer sensory preference for locally formulated complementary food formulae. *Food Science and Nutrition* 2018:1–8. doi: 10.1002/fsn3.856.

An, Y.-J., C.-F. Guo, M. Zhang, and Z.-P. Zhong. 2019. Investigation on characteristics of 3D printing using *Nostoc sphaeroides* biomass. *Journal of the Science of Food and Agriculture* 99 (2):639–46. doi: 10.1002/jsfa.9226.

Anukiruthika, T., J. Moses, and C. Anandharamakrishnan. 2019. Optimization of suitable post-processing method for 3D printed egg. *International Journal of Chemical Studies* 7:278–83.

Anukiruthika, T., J. Moses, and C. Anandharamakrishnan. 2020. 3D printing of egg yolk and white with rice flour blends. *Journal of Food Engineering* 265:109691. doi: 10.1016/j.jfoodeng.2019.109691.

Azam, R., M. Zhang, B. Bhandari, and C. Yang. 2018. Effect of different gums on features of 3d printed object based on vitamin-d enriched orange concentrate. *Food Biophysics* 13 (3):250–62. doi: 10.1007/s11483-018-9531-x.

Azam, S., M. Zhang, A. Mujumdar, and C. Yang. 2018. Study on 3D printing of orange concentrate and material characteristics. *Journal of Food Process Engineering* 41 (5):e12689. doi: 10.1111/jfpe.12689.

Balasubramanian, S., J. Kaur, and D. Singh. 2014. Optimization of weaning mix based on malted and extruded pearl millet and barley. *Journal of Food Science and Technology* 51 (4):682–90. doi: 10.1007/s13197-011-0579-6.

Bationo, F., C. Humblot, L. Songré-Ouattara, F. Hama-Ba, M. Le Merrer, M. Chapron, S. Kariluoto, and Y. Hemery. 2020. Total folate in West African cereal-based fermented foods: Bioaccessibility and influence of processing. *Journal of Food Composition and Analysis* 85:103309. doi: 10.1016/j.jfca.2019.103309.

Bolarinwa, I., P. Lim, and M. Kharidah. 2019. Quality of gluten-free cookies from germinated brown rice flour. *Food Research* 3 (3):199–207. doi: 10.26656/fr.2017.3(3).228.

Brückner-Gühmann, M., M. Banovic, and S. Drusch. 2019. Towards an increased plant protein intake: Rheological properties, sensory perception and consumer acceptability of lactic acid fermented, oat-based gels. *Food Hydrocolloids* 96:201–8. doi: 10.1016/j.foodhyd.2019.05.016.

byFlow. 2021. A 3D printer for food! Wait, what? https://www.3dbyflow.com/. Accessed March 20, 2021.

Carolo, L. 2020. Top 10 open-source 3D printers. https://all3dp.com/2/open-source-3d-printer-designs/. Accessed March 20, 2021.

Caulier, S., E. Doets, and M. Noort. 2020. An exploratory consumer study of 3D printed food perception in a real-life military setting. *Food Quality and Preference* 86:104001. doi: 10.1016/j.foodqual.2020.104001.

Chen, C.,. M. Zhang, C. Guo, and H. Chen. 2021. 4D printing of lotus root powder gel: Color change induced by microwave. *Innovative Food Science & Emerging Technologies* 68:102605. doi: 10.1016/j.ifset.2021.102605.

Chen, H., F. Xie, L. Chen, and B. Zheng. 2019. Effect of rheological properties of potato, rice and corn starches on their hot extrusion 3D printing behaviors. *Journal of Food Engineering* 244:150–8. doi: 10.1016/j.jfoodeng.2018.09.011.

Chen, J., T. Mu, D. Goffin, C. Blecker, G. Richard, A. Richel, and E. Haubruge. 2019. Application of soy protein isolate and hydrocolloids based mixtures as promising food material in 3D food printing. *Journal of Food Engineering* 261:76–86. doi: 10.1016/j.jfoodeng.2019.03.016.

Chen, J., M. Zhang, S. Devahastin, and D. Yu. 2021. Novel alternative use of near-infrared spectroscopy to indirectly forecast 3D printability of purple sweet potato pastes. *Journal of Food Engineering* 296:110464. doi: 10.1016/j.jfoodeng.2020.110464.

Chen, Y., M. Zhang, and P. Phuhongsung. 2021. 3D printing of protein-based composite fruit and vegetable gel system. *LWT - Food Science and Technology* 141:110978. doi: 10.1016/j.lwt.2021.110978.

Chinma, C.,. S. Azeez, H. Sulayman, K. Alhassan, S. Alozie, H. Gbadamosi, N. Danbaba, H. Oboh, J. Anuonye, and O. Adebo. 2020. Evaluation of fermented African yam bean flour composition and influence of substitution levels on properties of wheat bread. *Journal of Food Science* 85 (12):4281–9. doi: 10.1111/1750-3841.15527.

Chinma, C.,. J. Abu, B. Asikwe, T. Sunday, and O. Adebo. 2021. Effect of germination on the physicochemical, nutritional, functional, thermal properties and *in vitro* digestibility of Bambara groundnut flours. *LWT - Food Science and Technology* 140:110749. doi: 10.1016/j.lwt.2020.110749.

Cho, H.-D., H.-J. Min, Y.-S. Won, H.-Y. Ahn, Y.-S. Cho, and K.-I. Seo. 2019. Solid state fermentation process with *Aspergillus kawachii* enhances the cancer-suppressive potential of silkworm larva in hepatocellular carcinoma cells. *BMC Complementary and Alternative Medicine* 19 (1):241. doi: 10.1186/s12906-019-2649-7.

Cho, J., H. Zhao, J. Kim, S. Kim, and C. Chung. 2018. Characteristics of fermented seasoning sauces using *Tenebrio molitor* larvae. *Innovative Food Science & Emerging Technologies* 45:186–95. doi: 10.1016/j.ifset.2017.10.010.

Cohen, D., J. Lipton, M. Cutler, D. Coulter, A. Vesco, and H. Lipson. 2009. Hydrocolloid printing: a novel platform for customized food production. Proceedings of the 20th Annual International Solid Freeform Fabrication Symposium, pp. 807–818. Austin, TX.

Cosenza, G., S. Williams, D. Johnson, C. Sims, and C. McGowan. 2003. Development and evaluation of a fermented cabrito snack stick product. *Meat Science* 64 (1):51–7. doi: 10.1016/S0309-1740(02)00147-X.

Costa, K., M. Garcia, K. Ribeiro, M. Soares Junior, and M. Caliari. 2016. Rheological properties of fermented rice extract with probiotic bacteria and different concentrations of waxy maize starch. *LWT - Food Science and Technology* 72:71–7. doi: 10.1016/j.lwt.2016.04.014.

Daffner, K., S. Vadodaria, L. Ong, S. Nöbel, S. Gras, I. Norton, and T. Mills. 2021. Design and characterization of casein–whey protein suspensions via the pH–temperature-route for application in extrusion-based 3D-Printing. *Food Hydrocolloids* 112:105850 doi: 10.1016/j.foodhyd.2020.105850.

Dallagnol, A., M. Pescuma, G. De Valdez, and G. Rollán. 2013. Fermentation of quinoa and wheat slurries by *Lactobacillus plantarum* CRL 778: Proteolytic activity. *Applied Microbiology and Biotechnology* 97 (7):3129–40. doi: 10.1007/s00253-012-4520-3.

Dankar, I., A. Haddarah, F. E. L. Omar, F. Sepulcre, and M. Pujolà. 2018. 3D printing technology: The new era for food customization and elaboration. *Trends in Food Science & Technology* 75:231–42. doi: 10.1016/j.tifs.2018.03.018.

Dankar, I., M. Pujolá, F. El Omar, F. Sepulcre, and A. Haddarah. 2018. Impact of mechanical and microstructural properties of potato puree-food additive complexes on extrusion-based 3d printing. *Food and Bioprocess Technology* 11 (11):2021–31. doi: 10.1007/s11947-018-2159-5.

Dankar, I., A. Haddarah, F. Sepulcre, and M. Pujolá. 2020. Assessing mechanical and rheological properties of potato puree: Effect of different ingredient combinations and cooking methods on the feasibility of 3d printing. *Foods* 9 (1):21. doi: 10.3390/foods9010021.

Derossi, A., R. Caporizzi, D. Azzollini, and C. Severini. 2018. Application of 3D printing for customized food. A case on the development of a fruit-based snack for children. *Journal of Food Engineering* 220:65–75. doi: 10.1016/j.jfoodeng.2017.05.015.

Derossi, A., R. Caporizzi, L. Ricci, and C. Severini. 2019. Critical variables in 3D food printing. In *Fundamentals of 3D food printing and applications*, F. C. Godoi, B. R. Bhandari, S. Prakash, and M. Zhang, 41–91. London, UK: Academic Press. doi: 10.1016/B978-0-12-814564-7.00003-1.

Derossi, A., A. Husain, R. Caporizzi, and C. Severini. 2020. Manufacturing personalized food for people uniqueness. An overview from traditional to emerging technologies. *Critical Reviews in Food Science and Nutrition* 60 (7):1141–59. doi: 10.1080/10408398.2018.1559796.

Derossi, A., R. Paolillo, C. Caporizzi, and C. Severini. 2020. Extending the 3D food printing tests at high speed. Material deposition and effect of non-printing movements on the final quality of printed structures. *Journal of Food Engineering* 275:109865. doi: 10.1016/j.jfoodeng.2019.109865.

Derossi, A., R. Caporizzi, M. Paolillo, and C. Severini. 2021. Programmable texture properties of cereal-based snack mediated by 3D printing technology. *Journal of Food Engineering* 289:110160. doi: 10.1016/j.jfoodeng.2020.110160.

Diañez, I., C. Gallegos, E. Brito-de la Fuente, I. Martínez, C. Valencia, M. C. Sánchez, M. J. Diaz, and J. M. Franco. 2019. 3D printing in situ gelification of κ-carrageenan solutions: Effect of printing variables on the rheological response. *Food Hydrocolloids* 87:321–30. doi: 10.1016/j.foodhyd.2018.08.010.

Diaz, J., K. Van Bommel, M. Noort, J. Henket, and P. Briër. 2018. Method for the production of edible objects using sls and food products. Google patents.

Dick, A., B. Bhandari, and S. Prakash. 2019. Post-processing feasibility of composite-layer 3D printed beef. *Meat Science* 153:9–18. doi: 10.1016/j.meatsci.2019.02.024.

Dong, M.-Z., J.-Y. An, L.-T. Wang, X.-H. Fan, M.-J. Lv, Y.-W. Zhu, Y.-H. Chang, D. Meng, Q. Yang, and Y.-J. Fu. 2020. Development of fermented chestnut with *Bacillus natto*: Functional and sensory properties. *Food Research International (Ottawa, Ont.)* 130:108941 doi: 10.1016/j.foodres.2019.108941.

Dong, X., Y. Pan, W. Zhao, Y. Huang, W. Qu, J. Pan, H. Qi, and S. Prakash. 2020. Impact of microbial transglutaminase on 3D printing quality of *Scomberomorus niphonius* surimi. *LWT - Food Science and Technology* 124:109123. doi: 10.1016/j.lwt.2020.109123.

Emergen Research. 2020. Global fermented food and ingredients market 2017-2027. Report ID: ER_00375, 250 pp.

Emergen Research. 2021. 3D Food Printing Market Size to Reach USD 1,015.4 Million in 2027. https://www.globenewswire.com/news-release/2021/03/10/2190536/0/en/3D-Food-Printing-Market-Size-to-Reach-USD-1-015-4-Million-in-2027-Rising-Demand-for-Customized-Food-Products-and-Increasing-Adoption-in-Various-End-Use-Industries-are-Some-Key-Fact.html. Accessed March 21, 2021.

Fahmy, A., T. Becker, and M. Jekle. 2020. 3D printing and additive manufacturing of cereal-based materials: Quality analysis of starch-based systems using a camera-based morphological approach. *Innovative Food Science & Emerging Technologies* 63:102384. doi: 10.1016/j.ifset.2020.102384.

Fan, H., M. Zhang, Z. Liu, and Y. Ye. 2020. Effect of microwave-salt synergetic pre-treatment on the 3D printing performance of SPI-strawberry ink system. *LWT - Food Science and Technology* 122:109004. doi: 10.1016/j.lwt.2019.109004.

Feng, C., M. Zhang, B. Bhandari, and Y. Ye. 2020. Use of potato processing by-product: Effects on the 3D printing characteristics of the yam and the texture of air-fried yam snacks. *LWT - Food Science and Technology* 125:109265. doi: 10.1016/j.lwt.2020.109265.

Feng, L., J. Wu, J. Song, D. Li, Z. Zhang, Y. Xu, R. Yang, C. Liu, and M. Zhang. 2021. Effect of particle size distribution on the carotenoids release, physicochemical properties and 3D printing characteristics of carrot pulp. *LWT - Food Science and Technology* 139:110576. doi: 10.1016/j.lwt.2020.110576.

FoodBot 3D. 2021. Foodbot 3D food printer hot sale 2021. https://foodbot.en.made-in-china.com/product/LKlxgvRHXOUq/China-Foodbot-3D-Food-Printer-Hot-Sale-2021.html. Accessed March 20, 2021.

Gabriele, M., F. Sparvoli, R. Bollini, V. Lubrano, V. Longo, and L. Pucci. 2019. The impact of sourdough fermentation on non-nutritive compounds and antioxidant activities of flours from different *Phaseolus Vulgaris* L. genotypes. *Journal of Food Science* 84 (7):1929–36. doi: 10.1111/1750-3841.14672.

Gadallah, M., and M. Hassan. 2019. Quality properties of *Kishk* (a dried fermented cereal-milk mixture) prepared from different raw materials. *Journal of the Saudi Society of Agricultural Sciences* 18 (1):95–101. doi: 10.1016/j.jssas.2017.02.003.

García-Segovia, P., V. García-Alcaraz, S. Balasch-Parisi, and J. Martínez-Monzó. 2020. 3D printing of gels based on xanthan/konjac gums. *Innovative Food Science & Emerging Technologies* 64:102343. doi: 10.1016/j.ifset.2020.102343.

Garzón, A., M. Erben, C. Osella, and S. Drago. 2020. Effects of baking on γ-aminobutyric acid and free phenolic acids from gluten-free cookies made with native and malted whole sorghum flours. *Journal of Food Processing and Preservation* 44 (8):e14571. doi: 10.1111/jfpp.14571.

Ghazal, A., M. Zhang, and Z. Liu. 2019. Spontaneous color change of 3D printed healthy food product over time after printing as a novel application for 4D food printing. *Food and Bioprocess Technology* 12 (10):1627–45. doi: 10.1007/s11947-019-02327-6.

Ghazal, A., M. Zhang, B. Bhandari, and H. Chen. 2021. Investigation on spontaneous 4D changes in color and flavor of healthy 3D printed food materials over time in response to external or internal pH stimulus. *Food Research International (Ottawa, Ont.)* 142:110215. doi: 10.1016/j.foodres.2021.110215.

Gholamipour-Shirazi, A., I. Norton, and T. Mills. 2019. Designing hydrocolloid based food-ink formulations for extrusion 3D printing. *Food Hydrocolloids* 95:161–7. doi: 10.1016/j.foodhyd.2019.04.011.

Gong, L., W. Cao, H. Chi, J. Wang, H. Zhang, J. Liu, and B. Sun. 2018. Whole cereal grains and potential health effects: Involvement of the gut microbiota. *Food Research International (Ottawa, Ont.)* 103:84–102. doi: 10.1016/j.foodres.2017.10.025.

Gudjónsdóttir, M., R. Napitupulu, and H. Kristinsson. 2019. Low field NMR for quality monitoring of 3D printed surimi from cod by-products: Effects of the pH-shift method compared with conventional washing. *Magnetic Resonance in Chemistry: MRC* 57 (9):638–48. doi: 10.1002/mrc.4855.

Guo, C., M. Zhang, and B. Bhandari. 2019a. Model building and slicing in food 3D printing processes: A Review. *Comprehensive Reviews in Food Science and Food Safety* 18 (4):1052–69. doi: 10.1111/1541-4337.12443.

Guo, C., M. Zhang, and B. Bhandari. 2019b. A comparative study between syringe-based and screw-based 3D food printers by computational simulation. *Computers and Electronics in Agriculture* 162:397–404. doi: 10.1016/j.compag.2019.04.032.

Guo, C., M. Zhang, and S. Devahastin. 2020. 3D extrusion-based printability evaluation of selected cereal grains by computational fluid dynamic simulation. *Journal of Food Engineering* 286:110113. doi: 10.1016/j.jfoodeng.2020.110113.

Guo, C., M. Zhang, and H. Chen. 2020. Suitability of low-field nuclear magnetic resonance (LF-NMR) combining with back propagation artificial neural network (BP-ANN) to predict printability of polysaccharide hydrogels 3D printing. *International Journal of Food Science & Technology* doi: 10.1111/ijfs.14844.

Guo, C., M. Zhang, and S. Devahastin. 2021. Improvement of 3D printability of buckwheat starch-pectin system via synergistic Ca2+-microwave pretreatment. *Food Hydrocolloids* 113:106483. doi: 10.1016/j.foodhyd.2020.106483.

Hamet, M., J. Piermaria, and A. Abraham. 2015. Selection of EPS-producing *Lactobacillus* strains isolated from *kefir* grains and rheological characterization of the fermented milks. *LWT - Food Science and Technology* 63 (1):129–35. doi: 10.1016/j.lwt.2015.03.097.

Hamilton, C., G. Alici, and M. In Het Panhuis. 2018. 3D printing vegemite and marmite: Redefining "breadboards". *Journal of Food Engineering* 220:83–8. doi: 10.1016/j.jfoodeng.2017.01.008.

Hao, L., S. Mellor, O. Seaman, J. Henderson, N. Sewell, and M. Sloan. 2010. Material characterisation and process development for chocolate additive layer manufacturing. *Virtual and Physical Prototyping* 5 (2):57–64. doi: 10.1080/17452751003753212.

He, C., M. Zhang, and C. Guo. 2020. 4D printing of mashed potato/purple sweet potato puree with spontaneous color change. *Innovative Food Science & Emerging Technologies* 59:102250. doi: 10.1016/j.ifset.2019.102250.

Hertafeld, E., C. Zhang, Z. Jin, A. Jakub, K. Russell, Y. Lakehal, K. Andreyeva, S. Bangalore, J. Mezquita, J. Blutinger, et al. 2019. Multi-material three-dimensional food printing with simultaneous infrared cooking. *3D Printing and Additive Manufacturing* 6 (1):13–9. doi: 10.1089/3dp.2018.0042.

Hua, W., L. Na, and Z. Dong. 2018. 3D food printing can help elder to digest and swallow foods. *Journal of the American College of Cardiology* 72 (16):C210. doi: 10.1016/j.jacc.2018.08.911.

Huang, M., M. Zhang, and B. Bhandari. 2019. Assessing the 3D printing precision and texture properties of brown rice induced by infill levels and printing variables. *Food and Bioprocess Technology* 12 (7):1185–96. doi: 10.1007/s11947-019-02287-x.

Huang, M., M. Zhang, B. Bhandari, and Y. Liu. 2020. Improving the three-dimensional printability of taro paste by the addition of additives. *Journal of Food Process Engineering* 43 (5):e13090. doi: 10.1111/jfpe.13090.

Jan, R., C. Saxena, and S. Singh. 2017. Effect of extrusion variables on antioxidant activity, total phenolic content and dietary fibre content of gluten-free extrudate from germinated Chenopodium (*Chenopodium album*) flour. *International Journal of Food Science & Technology* 52 (12):2623–30. doi: 10.1111/ijfs.13549.

Jan, R., D. Saxena, and S. Singh. 2018. Comparative study of raw and germinated Chenopodium (*Chenopodium album*) flour on the basis of thermal, rheological, minerals, fatty acid profile and phytocomponents. *Food Chemistry* 269:173–80. doi: 10.1016/j.foodchem.2018.07.003.

Jiménez, D., M. Lobo, B. Irigaray, M. Grompone, and N. Sammán. 2020. Oxidative stability of baby dehydrated purees formulated with different oils and germinated grain flours of quinoa and amaranth. *LWT - Food Science and Technology* 127:109229. doi: 10.1016/j.lwt.2020.109229.

Karyappa, R., and M. Hashimoto. 2019. Chocolate-based ink three-dimensional printing (Ci3DP). *Scientific Reports* 9 (1):14178. doi: 10.1038/s41598-019-50583-5.

Kewuyemi, Y., H. Kesa, C. Chinma, and O. Adebo. 2020. Fermented edible insects for promoting food security in Africa. *Insects* 11 (5):283. doi: 10.3390/insects11050283.

Kewuyemi, Y., P. Njobeh, E. Kayitesi, J. Adebiyi, A. Oyedeji, M. Adefisoye, and O. Adebo. 2020. Metabolite profile of whole grain *ting* (a Southern African fermented product) obtained using two strains of *Lactobacillus fermentum*. *Journal of Cereal Science* 95:103042. doi: 10.1016/j.jcs.2020.103042.

Kim, H., H. Bae, and H. Park. 2018. Reprint of classification of the printability of selected food for 3D printing: Development of an assessment method using hydrocolloids as reference material. *Journal of Food Engineering* 220:28–37. doi: 10.1016/j.jfoodeng.2017.10.023.

Kim, H., I. Lee, S. Park, J. Lee, M.-H. Nguyen, and H. Park. 2019. Effect of hydrocolloid addition on dimensional stability in post-processing of 3D printable cookie dough. *LWT - Food Science and Technology* 101:69–75. doi: 10.1016/j.lwt.2018.11.019.

Kira. 2015. EU develops PERFORMANCE 3D printed food for elderly and patients with dysphagia. http://www.3ders.org/articles/20151026-eu-develops-performance-3d-printed-food-for-elderly-and-patients-with-dysphagia.html. Accessed May 22, 2020.

Kouzani, A., S. Adams, D. Whyte, R. Oliver, B. Hemsley, S. Palmer, and S. Balandin. 2017. 3D printing of food for people with swallowing difficulties. *KnE Engineering* 2 (2):23–9. doi: 10.18502/keg.v2i2.591.

Krishnaraj, P., T. Anukiruthika, P. Choudhary, J. Moses, and C. Anandharamakrishnan. 2019. 3D extrusion printing and post-processing of fibre-rich snack from indigenous composite flour. *Food and Bioprocess Technology* 12 (10):1776–86. doi: 10.1007/s11947-019-02336-5.

Ktenioudaki, A., L. Alvarez-Jubete, T. Smyth, K. Kilcawley, D. Rai, and E. Gallagher. 2015. Application of bioprocessing techniques (sourdough fermentation and technological aids) for brewer's spent grain breads. *Food Research International* 73:107–16. doi: 10.1016/j.foodres.2015.03.008.

Lanaro, M., D. Forrestal, S. Scheurer, D. Slinger, S. Liao, S. Powell, and M. Woodruff. 2017. 3D printing complex chocolate objects: Platform design, optimization and evaluation. *Journal of Food Engineering* 215:13–22. doi: 10.1016/j.jfoodeng.2017.06.029.

Lansard, M. 2021. Food 3D printing: 7 food 3D printers available in 2021. https://www.aniwaa.com/buyers-guide/3d-printers/food-3d-printers/. Accessed March 20, 2021.

Le Tohic, C., J. J. O'Sullivan, K. P. Drapala, V. Chartrin, T. Chan, A. P. Morrison, J. P. Kerry, and A. L. Kelly. 2018. Effect of 3D printing on the structure and textural properties of processed cheese. *Journal of Food Engineering* 220:56–64. doi: 10.1016/j.jfoodeng.2017.02.003.

Le-Bail, A., B. Maniglia, and P. Le-Bail. 2020. Recent advances and future perspective in additive manufacturing of foods based on 3D printing. *Current Opinion in Food Science* 35:54–64. doi: 10.1016/j.cofs.2020.01.009.

Lee, J., D. Won, H. Kim, and H. Park. 2019. Effect of particle size on 3D printing performance of the food-ink system with cellular food materials. *Journal of Food Engineering* 256:1–8. doi: 10.1016/j.jfoodeng.2019.03.014.

Lille, M., A. Nurmela, E. Nordlund, S. Metsä-Kortelainen, and N. Sozer. 2018. Applicability of protein and fiber-rich food materials in extrusion-based 3D printing. *Journal of Food Engineering* 220:20–7. doi: 10.1016/j.jfoodeng.2017.04.034.

Lipson, H., and M. Kurman. 2013. Printing in layers. In *Fabricated: The new world of 3d printing: the new world of 3D printing*, eds. H. Lipson and M. Kurman, 65–84. Hoboken, NJ: John Wiley & Sons.

Lipton, J., D. Arnold, F. Nigl, N. Lopez, D. Cohen, N. Norén, and H. Lipson. 2010. Mutli-material food printing with complex internal structure suitable for conventional post-processing. Paper presented at the 21st Annual International Solid Freeform Fabrication (SFF) symposium, Texas, August 9–11, 2010, 809–15. http://sffsymposium.engr.utexas.edu/Manuscripts/2010/2010-68-Lipton.pdf.

Liu, C., C. Ho, and J. Wang. 2018. The development of 3D food printer for printing fibrous meat materials. Paper presented at the 2017 2nd International Conference on Innovative Engineering Materials (ICIEM 2017), Philadelphia, October, 21-26, 2017. doi: 10.1088/1757-899X/284/1/012019.

Liu, L.,. Y. Meng, X. Dai, K. Chen, and Y. Zhu. 2019. 3D printing complex egg white protein objects: Properties and optimization. *Food and Bioprocess Technology* 12 (2):267–79. doi: 10.1007/s11947-018-2209-z.

Liu, L.,. X. Yang, B. Bhandari, Y. Meng, and S. Prakash. 2020. Optimization of the formulation and properties of 3D-printed complex egg white protein objects. *Foods* 9 (2):164. doi: 10.3390/foods9020164.

Liu, Q., N. Zhang, W. Wei, X. Hu, Y. Tan, Y. Yu, Y. Deng, C. Bi, L. Zhang, and H. Zhang. 2020. Assessing the dynamic extrusion-based 3D printing process for power-law fluid using numerical simulation. *Journal of Food Engineering* 275:109861. doi: 10.1016/j.jfoodeng.2019.109861.

Liu, Y., D. Liu, G. Wei, Y. Ma, B. Bhandari, and P. Zhou. 2018. 3D printed milk protein food stimulant: Improving the printing performance of milk protein concentration by incorporating whey protein isolate. *Innovative Food Science & Emerging Technologies* 49:116–26. doi: 10.1016/j.ifset.2018.07.018.

Liu, Y., Y. Yu, C. Liu, J. Regenstein, X. Liu, and P. Zhou. 2019. Rheological and mechanical behavior of milk protein composite gel for extrusion-based 3D food printing. *LWT - Food Science and Technology* 102:338–46. doi: 10.1016/j.lwt.2018.12.053.

Liu, Y., W. Zhang, K. Wang, Y. Bao, J. Regenstein, and P. Zhou. 2019. Fabrication of gel-like emulsions with whey protein isolate using microfluidization: Rheological properties and 3d printing performance. *Food and Bioprocess Technology* 12 (12):1967–79. doi: 10.1007/s11947-019-02344-5.

Liu, Y., X. Liang, A. Saeed, W. Lan, and W. Qin. 2019. Properties of 3D printed dough and optimization of printing parameters. *Innovative Food Science & Emerging Technologies* 54:9–18. doi: 10.1016/j.ifset.2019.03.008.

Liu, Y., T. Tang, S. Duan, Z. Qin, H. Zhao, M. Wang, C. Li, Z. Zhang, A. Liu, G. Han, et al. 2020. Applicability of rice doughs as promising food materials in extrusion-based 3D printing. *Food and Bioprocess Technology* 13 (3):548–63. doi: 10.1007/s11947-020-02415-y.

Liu, Y., T. Tang, S. Duan, Z. Qin, C. Li, Z. Zhang, A. Liu, D. Wu, H. Chen, G. Han, et al. 2020. Effects of sodium alginate and rice variety on the physicochemical characteristics and 3D printing feasibility of rice paste. *LWT - Food Science and Technology* 127:109360. doi: 10.1016/j.lwt.2020.109360.

Liu, Z., and M. Zhang. 2019. 3D food printing technologies and factors affecting printing precision. In *Fundamentals of 3D food printing and applications*, eds. F. C. Godoi, B. R. Bhandari, S. Prakash, and M. Zhang, 19–40. London, UK: Academic Press. doi: 10.1016/B978-0-12-814564-7.00002-X.

Liu, Z., and M. Zhang. 2021. Texture properties of microwave post-processed 3D printed potato snack with different ingredients and infill structure. *Future Foods* 3:100017. doi: 10.1016/j.fufo.2021.100017.

Liu, Z., B. Bhandari, S. Prakash, and M. Zhang. 2018. Creation of internal structure of mashed potato construct by 3D printing and its textural properties. *Food Research International* 111:534–43. doi: 10.1016/j.foodres.2018.05.075.

Liu, Z., M. Zhang, and B. Bhandari. 2018. Effect of gums on the rheological, microstructural and extrusion printing characteristics of mashed potatoes. *International Journal of Biological Macromolecules* 117:1179–87. doi: 10.1016/j.ijbiomac.2018.06.048.

Liu, Z., M. Zhang, and C. Yang. 2018. Dual extrusion 3D printing of mashed potatoes/strawberry juice gel. *LWT - Food Science and Technology* 96:589–96. doi: 10.1016/j.lwt.2018.06.014.

Liu, Z., M. Zhang, B. Bhandari, and C. Yang. 2018. Impact of rheological properties of mashed potatoes on 3D printing. *Journal of Food Engineering* 220:76–82. doi: 10.1016/j.jfoodeng.2017.04.017.

Liu, Z., B. Bhandari, S. Prakash, S. Mantihal, and M. Zhang. 2019. Linking rheology and printability of a multicomponent gel system of carrageenan-xanthan-starch in extrusion based additive manufacturing. *Food Hydrocolloids* 87:413–24. doi: 10.1016/j.foodhyd.2018.08.026.

Liu, Z., B. Bhandari, and M. Zhang. 2020. Incorporation of probiotics (*Bifidobacterium animalis* subsp. Lactis) into 3D printed mashed potatoes: Effects of variables on the viability. *Food Research International (Ottawa, Ont.)* 128:108795. doi: 10.1016/j.foodres.2019.108795.

Liu, Z., A. Dick, S. Prakash, B. Bhandari, and M. Zhang. 2020. Texture modification of 3D printed air-fried potato snack by varying its internal structure with the potential to reduce oil content. *Food and Bioprocess Technology* 13 (3):564–76. doi: 10.1007/s11947-020-02408-x.

Liu, Z., M. Zhang, and Y. Ye. 2020. Indirect prediction of 3D printability of mashed potatoes based on LF-NMR measurements. *Journal of Food Engineering* 287:110137. doi: 10.1016/j.jfoodeng.2020.110137.

Liu, Z., H. Chen, B. Zheng, F. Xie, and L. Chen. 2020. Understanding the structure and rheological properties of potato starch induced by hot-extrusion 3D printing. *Food Hydrocolloids* 105:105812. doi: 10.1016/j.foodhyd.2020.105812.

Luo, Y.-W., W.-H. Xie, X.-X. Jin, Q. Wang, and Y.-J. He. 2014. Effects of germination on iron, zinc, calcium, manganese, and copper availability from cereals and legumes. *CyTA - Journal of Food* 12 (1):22–6. doi: 10.1080/19476337.2013.782071.

Mabotja, F., D. Metcalfe, and O. Adebo. 2021. South African consumers' interpretation of nutritional labelling systems of food products. *Transactions of the Royal Society of South Africa* 76 (1):41–51. doi: 10.1080/0035919x.2020.1834466.

Maniglia, B., D. Lima, M. Junior, P. Le-Bail, A. Le-Bail, and P. Augusto. 2019. Hydrogels based on ozonated cassava starch: Effect of ozone processing and gelatinization conditions on enhancing 3D-printing applications. *International Journal of Biological Macromolecules* 138:1087–97. doi: 10.1016/j.ijbiomac.2019.07.124.

Maniglia, B., D. Lima, M. Junior, P. Le-Bail, A. Le-Bail, and P. Augusto. 2020. Preparation of cassava starch hydrogels for application in 3D printing using dry heating treatment (DHT): A prospective study on the effects of DHT and gelatinization conditions. *Food Research International (Ottawa, Ont.)* 128:108803. doi: 10.1016/j.foodres.2019.108803.

Manstan, T., and M. McSweeney. 2020. Consumers' attitudes towards and acceptance of 3D printed foods in comparison with conventional food products. *International Journal of Food Science & Technology* 55 (1):323–31. doi: 10.1111/ijfs.14292.

Manstan, T., S. Chandler, and M. McSweeney. 2021. Consumers' attitudes towards 3D printed foods after a positive experience: An exploratory study. *Journal of Sensory Studies* 36 (1):e12619. doi: 10.1111/joss.12619.

Mantihal, S., S. Prakash, F. Godoi, and B. Bhandari. 2017. Optimization of chocolate 3D printing by correlating thermal and flow properties with 3D structure modeling. *Innovative Food Science & Emerging Technologies* 44:21–9. doi: 10.1016/j.ifset.2017.09.012.

Mantihal, S., S. Prakash, and B. Bhandari. 2019a. Texture-modified 3D printed dark chocolate: Sensory evaluation and consumer perception study. *Journal of Texture Studies* 50 (5):386–99. doi: 10.1111/jtxs.12472.

Mantihal, S., S. Prakash, and B. Bhandari. 2019b. Textural modification of 3D printed dark chocolate by varying internal infill structure. *Food Research International (Ottawa, Ont.)* 121:648–57. doi: 10.1016/j.foodres.2018.12.034.

Mantihal, S., S. Prakash, F. Godoi, and B. Bhandari. 2019. Effect of additives on thermal, rheological and tribological properties of 3D printed dark chocolate. *Food Research International (Ottawa, Ont.)* 119:161–9. doi: 10.1016/j.foodres.2019.01.056.

Martínez-Monzó, J., J. Cárdenas, and P. García-Segovia. 2019. Effect of temperature on 3D printing of commercial potato puree. *Food Biophysics* 14 (3):225–34. doi: 10.1007/s11483-019-09576-0.

Metcalf, D., K. Wiener, and A. Saliba. 2021. Comparing early hemp food consumers to non-hemp food consumers to determine attributes of early adopters of a novel food using the Food Choice Questionnaire (FCQ) and the Food Neophobia Scale (FNS). *Future Foods* 3:100031. doi: 10.1016/j.fufo.2021.100031.

Mosso, A., J. LeBlanc, C. Motta, I. Castanheira, P. Ribotta, and N. Sammán. 2020. Effect of fermentation in nutritional, textural and sensorial parameters of vegan-spread products using a probiotic folate-producing *Lactobacillus sakei* strain. *LWT - Food Science and Technology* 127:109339. doi: 10.1016/j.lwt.2020.109339.

Natural Machines. 2021. Foodini natural machines. https://www.naturalmachines.com/foodini. Accessed March 20, 2021.

Nelson, K., M. Mathai, J. Ashton, O. Donkor, T. Vasiljevic, R. Mamilla, and L. Stojanovska. 2016. Effects of malted and non-malted wholegrain wheat on metabolic and inflammatory biomarkers in overweight/obese adults: A randomized crossover pilot study. *Food Chemistry* 194:495–502. doi: 10.1016/j.foodchem.2015.08.023.

Nijdam, J., D. Agarwal, and B. Schon. 2021. Assessment of a novel window of dimensional stability for screening food inks for 3D printing. *Journal of Food Engineering* 292:110349. doi: 10.1016/j.jfoodeng.2020.110349.

Nijdam, J., D. LeCorre-Bordes, A. Delvart, and B. Schon. 2021. A rheological test to assess the ability of food inks to form dimensionally stable 3D food structures. *Journal of Food Engineering* 291:110235. doi: 10.1016/j.jfoodeng.2020.110235.

Obilana, A., B. Odhav, and V. Jideani. 2018. Nutritional, biochemical and sensory properties of instant beverage powder made from two different varieties of pearl millet. *Food and Nutrition Research* 62:1524. doi: 10.29219/fnr.v62.1524.

Ocheme, O., and C. Chinma. 2008. Effects of soaking and germination on some physicochemical properties of millet flour for porridge production. *Journal of Food Technology* 6:185–8.

Ohanenye, I., A. Tsopmo, C. Ejike, and C. Udenigwe. 2020. Germination as a bioprocess for enhancing the quality and nutritional prospects of Legume proteins. *Trends in Food Science & Technology* 101:213–22. doi: 10.1016/j.tifs.2020.05.003.

Ojijo, N., and E. Shimoni. 2004. Rheological properties of fermented finger millet (*Eleucine coracana*) thin porridge. *Carbohydrate Polymers* 57 (2):135–43. doi: 10.1016/j.carbpol.2004.02.011.

Olojede, A., A. Sanni, and K. Banwo. 2020. Rheological, textural and nutritional properties of gluten-free sourdough made with functionally important lactic acid bacteria and yeast from Nigerian sorghum. *LWT - Food Science and Technology* 120:108875. doi: 10.1016/j.lwt.2019.108875.

Oranusi, S., and S. O. Dahunsi. 2015. Preliminary study on hazards and critical control points of kokoro, a Nigerian indigenous fermented maize snack. *SpringerPlus* 4 (1):253. doi: 10.1186/s40064-015-1026-3.

Oyeyinka, S., O. Akintayo, O. Adebo, E. Kayitesi, and P. Njobeh. 2021. A review on the physicochemical properties of starches modified by microwave alone and in combination with other methods. *International Journal of Biological Macromolecules* 176:87–95. doi: 10.1016/j.ijbiomac.2021.02.066.

Oyinloye, T., and W. Yoon. 2021. Stability of 3D printing using a mixture of pea protein and alginate: Precision and application of additive layer manufacturing simulation approach for stress distribution. *Journal of Food Engineering* 288:110127. doi: 10.1016/j.jfoodeng.2020.110127.

Pant, A., A. Lee, R. Karyappa, C. Lee, J. An, M. Hashimoto, U. Tan, G. Wong, C. Chua, and Y. Zhang. 2021. 3D food printing of fresh vegetables using food hydrocolloids for dysphagic patients. *Food Hydrocolloids* 114:106546. doi: 10.1016/j.foodhyd.2020.106546.

Paolillo, M., A. Derossi, K. van Bommel, M. Noort, and C. Severini. 2021. Rheological properties, dispensing force and printing fidelity of starchy-gels modulated by concentration, temperature and resting time. *Food Hydrocolloids* 117:106703. doi: 10.1016/j.foodhyd.2021.106703.

Park, S., H. Kim, and H. Park. 2020. Callus-based 3D printing for food exemplified with carrot tissues and its potential for innovative food production. *Journal of Food Engineering* 271:109781. doi: 10.1016/j.jfoodeng.2019.109781.

Paxton, N., W. Smolan, T. Böck, F. Melchels, J. Groll, and T. Jungst. 2017. Proposal to assess printability of bioinks for extrusion-based bioprinting and evaluation of rheological properties governing bioprintability. *Biofabrication* 9 (4):044107. doi: 10.1088/1758-5090/aa8dd8.

Pérez, B., H. Nykvist, A. Brøgger, M. Larsen, and M. Falkeborg. 2019. Impact of macronutrients printability and 3D-printer parameters on 3D-food printing: A review. *Food Chemistry* 287:249–57. doi: 10.1016/j.foodchem.2019.02.090.

Phuhongsung, P.,. M. Zhang, and S. Devahastin. 2020. Investigation on 3D printing ability of soybean protein isolate gels and correlations with their rheological and textural properties via LF-NMR spectroscopic characteristics. *LWT - Food Science and Technology* 122:109019. doi: 10.1016/j.lwt.2020.109019.

Piyush, Kumar, R., Kumar. and R. 2020. 3D printing of food materials: A state of art review and future applications. *Materials Today: Proceedings*, in press. doi: 10.1016/j.matpr.2020.02.005.

Pliner, P., and K. Hobden. 1992. Development of a scale to measure the trait of food neophobia in humans. *Appetite* 19 (2):105–20. doi: 10.1016/0195-6663(92)90014-W.

Polat, H., T. Capar, C. Inanir, L. Ekici, and H. Yalcin. 2020. Formulation of functional crackers enriched with germinated lentil extract: A response surface methodology Box-Behnken design. *LWT - Food Science and Technology* 123:109065. doi: 10.1016/j.lwt.2020.109065.

Portanguen, S., P. Tournayre, J. Sicard, T. Astruc, and P.-S. Mirade. 2019. Toward the design of functional foods and biobased products by 3D printing: A review. *Trends in Food Science & Technology* 86:188–98. doi: 10.1016/j.tifs.2019.02.023.

Pulatsu, E., J.-W. Su, J. Lin, and M. Lin. 2020. Factors affecting 3D printing and post-processing capacity of cookie dough. *Innovative Food Science & Emerging Technologies* 61:102316. doi: 10.1016/j.ifset.2020.102316.

Pulatsu, E., and M. Lin. 2021. A review on customizing edible food materials into 3D printable inks: Approaches and strategies. *Trends in Food Science & Technology* 107:68–77. doi: 10.1016/j.tifs.2020.11.023.

Rizzello, C., B. Hernández-Ledesma, S. Fernández-Tomé, J. Curiel, D. Pinto, B. Marzani, R. Coda, and M. Gobbetti. 2015. Italian legumes: Effect of sourdough fermentation on lunasin-like polypeptides. *Microbial Cell Factories* 14:168. doi: 10.1186/s12934-015-0358-6.

Rodgers, S. 2016. Minimally processed functional foods: Technological and operational pathways. *Journal of Food Science* 81 (10): R2309–R2319. doi: 10.1111/1750-3841.13422.

Roncolini, A., V. Milanović, L. Aquilanti, F. Cardinali, C. Garofalo, R. Sabbatini, F. Clementi, L. Belleggia, M. Pasquini, M. Mozzon, et al. 2020. Lesser mealworm (*Alphitobius diaperinus*) powder as a novel baking ingredient for manufacturing high-protein, mineral-dense snacks. *Food Research International (Ottawa, Ont.)* 131:109031. doi: 10.1016/j.foodres.2020.109031.

Schutyser, M., S. Houlder, M. de Wit, C. Buijsse, and A. Alting. 2018. Fused deposition modelling of sodium caseinate dispersions. *Journal of Food Engineering* 220:49–55. doi: 10.1016/j.jfoodeng.2017.02.004.

Setia, R., Z. Dai, M. Nickerson, E. Sopiwnyk, L. Malcolmson, and Y. Ai. 2019. Impacts of short-term germination on the chemical compositions, technological characteristics and nutritional quality of yellow pea and faba bean flours. *Food Research International (Ottawa, Ont.)* 122:263–72. doi: 10.1016/j.foodres.2019.04.021.

Savastano, M., C. Amendola, and F. D'Ascenzo. 2018. How digital transformation is reshaping the manufacturing industry value chain: The new digital manufacturing ecosystem applied to a case study from the food industry, Lecture Notes in Information Systems and Organization. In *Network, smart and open*, eds. R. Lamboglia, A. Cardoni, R. Dameri, and D. Mancini, 127–42. Basel, Switzerland: Springer. doi: 10.1007/978-3-319-62636-9_9.

Severini, C., A. Derossi, and D. Azzollini. 2016. Variables affecting the printability of foods: Preliminary tests on cereal-based products. *Innovative Food Science & Emerging Technologies* 38:281–91. doi: 10.1016/j.ifset.2016.10.001.

Severini, C., D. Azzollini, M. Albenzio, and A. Derossi. 2018. On printability, quality and nutritional properties of 3D printed cereal based snacks enriched with edible insects. *Food Research International (Ottawa, Ont.)* 106:666–76. doi: 10.1016/j.foodres.2018.01.034.

Severini, C., A. Derossi, I. Ricci, R. Caporizzi, and A. Fiore. 2018. Printing a blend of fruit and vegetables. New advances on critical variables and shelf life of 3D edible objects. *Journal of Food Engineering* 220:89–100. doi: 10.1016/j.jfoodeng.2017.08.025.

Singh, A., and S. Sharma. 2017. Bioactive components and functional properties of biologically activated cereal grains: A bibliographic review. *Critical Reviews in Food Science and Nutrition* 57 (14): 3051–71. doi: 10.1080/10408398.2015.1085828.

Sobowale, S.,. O. Animashaun, A. Mulaba-Bafubiandi, T. Abidoye, Y. Kewuyemi, and O. Adebo. 2018. Process optimization of extrusion variables and its effect on properties of extruded cocoyam (*Xanthosoma sagittifolium*) noodles. *Food Science & Nutrition* 6 (8): 2210–26. doi: 10.1002/fsn3.786.

Sun, J., W. Zhou, L. Yan, D. Huang, and L. Lin. 2018. Extrusion-based food printing for digitalized food design and nutrition control. *Journal of Food Engineering* 220:1–11. doi: 10.1016/j.jfoodeng.2017.02.028.

Tamang, J., P. Cotter, A. Endo, N. Han, R. Kort, S. Liu, B. Mayo, N. Westerik, and R. Hutkins. 2020. Fermented foods in a global age: East meets West. *Comprehensive Reviews in Food Science and Food Safety* 19 (1):184–217. doi: 10.1111/1541-4337.12520.

Taylor, J., and J. Taylor. 2017. Proteins from sorghum and millets. In *Sustainable protein sources*, eds. S. R. Nadathur, J. P. D. Wanasundara, and L. Scanlin, 79–104. Amsterdam, the Netherlands: Elsevier. doi: 10.1016/B978-0-12-802778-3.00005-6.

Theagarajan, R., J. A. Moses, and C. Anandharamakrishnan. 2020. 3D extrusion printability of rice starch and optimization of process variables. *Food and Bioprocess Technology* 13 (6):1048–62. doi: 10.1007/s11947-020-02453-6.

Theodoridis, G., A. Pechlivanis, N. Thomaidis, A. Spyros, C. Georgiou, T. Albanis, I. Skoufos, S. Kalogiannis, G. Tsangaris, A. Stasinakis, et al. 2021. FoodOmicsGR_RI: A consortium for comprehensive molecular characterisation of food products. *Metabolites* 11 (2):74. doi: 10.3390/metabo11020074.

Theodoro, J., O. Martinez, M. Grancieri, R. Toledo, A. Dias Martins, D. Dias, C. Wanderlei, P. Carvalho, and H. Martino. 2021. Germinated millet flour (Pennisetum glaucum (L.) R. Br.) reduces inflammation, oxidative stress, and liver steatosis in rats fed with high-fat high-fructose diet. *Journal of Cereal Science* 99:103207. doi: 10.1016/j.jcs.2021.103207.

Thorsen, L., W. Abdelgadir, M. Rønsbo, S. Abban, S. Hamad, D. Nielsen, and M. Jakobsen. 2011. Identification and safety evaluation of *Bacillus* species occurring in high numbers during spontaneous fermentations to produce *Gergoush*, a traditional Sudanese bread snack. *International Journal of Food Microbiology* 146 (3):244–52. doi: 10.1016/j.ijfoodmicro.2011.02.028.

Torrico, D., S. Fuentes, C. Viejo, H. Ashman, and F. Dunshea. 2019. Cross-cultural effects of food product familiarity on sensory acceptability and non-invasive physiological responses of consumers. *Food Research International (Ottawa, Ont.)* 115:439–50. doi: 10.1016/j.foodres.2018.10.054.

Tuorila, H., and C. Hartmann. 2020. Consumer responses to novel and unfamiliar foods. *Current Opinion in Food Science* 33:1–8. doi: 10.1016/j.cofs.2019.09.004s.

Vancauwenberghe, V.,. L. Katalagarianakis, Z. Wang, M. Meerts, M. Hertog, P. Verboven, P. Moldenaers, M. E. Hendrickx, J. Lammertyn, and B. Nicolaï. 2017. Pectin based food-ink formulations for 3-D printing of customizable porous food stimulants. *Innovative Food Science & Emerging Technologies* 42:138–50. doi: 10.1016/j.ifset.2017.06.011.

Vancauwenberghe, V.,. P. Verboven, J. Lammertyn, and B. Nicolaï. 2018. Development of a coaxial extrusion deposition for 3D printing of customizable pectin-based food stimulant. *Journal of Food Engineering* 225:42–52. doi: 10.1016/j.jfoodeng.2018.01.008.

Vancauwenberghe, V.,. M. A. Delele, J. Vanbiervliet, W. Aregawi, P. Verboven, J. Lammertyn, and B. Nicolaï. 2018. Model-based design and validation of food texture of 3D printed pectin-based food stimulants. *Journal of Food Engineering* 231:72–82. doi: 10.1016/j.jfoodeng.2018.03.010.

Väkeväinen, K., F. Ludena-Urquizo, E. Korkala, A. Lapveteläinen, S. Peräniemi, A. von Wright, and C. Plumed-Ferrer. 2020. Potential of quinoa in the development of fermented spoonable vegan products. *LWT - Food Science and Technology* 120:108912. doi: 10.1016/j.lwt.2019.108912.

Verni, M., V. Verardo, and C. G. Rizzello. 2019. How fermentation affects the antioxidant properties of cereals and legumes. *Foods* 8 (9):362. doi: 10.3390/foods8090362.

Wang, L., M. Zhang, B. Bhandari, and C. Yang. 2018. Investigation on fish surimi gel as promising food material for 3D printing. *Journal of Food Engineering* 220:101–8. doi: 10.1016/j.jfoodeng.2017.02.029.

Warner, E., I. Norton, and T. Mills. 2019. Comparing the viscoelastic properties of gelatin and different concentrations of kappa-carrageenan mixtures for additive manufacturing applications. *Journal of Food Engineering* 246:58–66. doi: 10.1016/j.jfoodeng.2018.10.033.

Wójtowicz, A., and L. Mościcki. 2014. Influence of legume type and addition level on quality characteristics, texture and microstructure of enriched precooked pasta. *LWT - Food Science and Technology* 59 (2):1175–85. doi: 10.1016/j.lwt.2014.06.010.

Xiang, H., D. Sun-Waterhouse, G. I. N. Waterhouse, C. Cui, and Z. Ruan. 2019. Fermentation-enabled wellness foods: A fresh perspective. *Food Science and Human Wellness* 8 (3):203–43. doi: 10.1016/j.fshw.2019.08.003.

Xu, K., M. Zhang, and B. Bhandari. 2020. Effect of novel ultrasonic-microwave combined pretreatment on the quality of 3D printed wheat starch-papaya system. *Food Biophysics* 15 (2):249–60. doi: 10.1007/s11483-019-09615-w.

Xu, L., L. Gu, Y. Su, C. Chang, J. Wang, S. Dong, Y. Liu, Y. Yang, and J. Li. 2020. Impact of thermal treatment on the rheological, microstructural, protein structures and extrusion 3D printing characteristics of egg yolk. *Food Hydrocolloids* 100:105399. doi: 10.1016/j.foodhyd.2019.105399.

Yağci, S., A. Altan, and F. Doğan. 2020. Effects of extrusion processing and gum content on physicochemical, microstructural and nutritional properties of fermented chickpea-based extrudates. *LWT - Food Science and Technology* 124:109150. doi: 10.1016/j.lwt.2020.109150.

Yang, F., M. Zhang, S. Prakash, and Y. Liu. 2018. Physical properties of 3D printed baking dough as affected by different compositions.

Innovative Food Science & Emerging Technologies 49:202–10. doi: 10.1016/j.ifset.2018.01.001.

Yang, F., M. Zhang, Z. Fang, and Y. Liu. 2019. Impact of processing parameters and post-treatment on the shape accuracy of 3D-printed baking dough. *International Journal of Food Science & Technology* 54 (1):68–74. doi: 10.1111/ijfs.13904.

Yang, F., M. Zhang, and Y. Liu. 2019. Effect of post-treatment microwave vacuum drying on the quality of 3D-printed mango juice gel. *Drying Technology* 37 (14):1757–65. doi: 10.1080/07373937.2018.1536884.

Yang, F., M. Zhang, B. Bhandari, and Y. Liu. 2018. Investigation on lemon juice gel as food material for 3D printing and optimization of printing parameters. *LWT - Food Science and Technology* 87:67–76. doi: 10.1016/j.lwt.2017.08.054.

Yang, F., C. Guo, M. Zhang, B. Bhandari, and Y. Liu. 2019. Improving 3D printing process of lemon juice gel based on fluid flow numerical simulation. *LWT - Food Science and Technology* 102:89–99. doi: 10.1016/j.lwt.2018.12.031.

Yue, Q., M. Li, C. Liu, L. Li, X. Zheng, and K. Bian. 2020. Extensional rheological properties in mixed and fermented/rested dough and relationships with steamed bread quality. *Journal of Cereal Science* 93:102968. doi: 10.1016/j.jcs.2020.102968.

Zhang, L., Y. Lou, and M. A. I. Schutyser. 2018. 3D printing of cereal-based food structures containing probiotics. *Food Structure* 18:14–22. doi: 10.1016/j.foostr.2018.10.002.

Zhou, Q., M. Wang, H. Li, S. Wang, W. Sun, X. Chen, L. Dong, and Z. Ruan. 2020. Application of maillard reaction product of xylose-pea protein enzymatic hydrolysate in 3D printing. *Journal of the Science of Food and Agriculture* 100 (7):2982–90. doi: 10.1002/jsfa.10327.

Zhu, J., Y. Chen, C. Lv, W. Wu, and S. Qin. 2019. Study on optimization of removing cadmium by lactobacillus fermentation and its effect on physicochemical and quality properties of rice noodles. *Food Control* 106:106740. doi: 10.1016/j.foodcont.2019.106740.

Zhu, S., M. A. Stieger, A. J. van der Goot, and M. A. I. Schutyser. 2019. Extrusion-based 3D printing of food pastes: Correlating rheological properties with printing behavior. *Innovative Food Science & Emerging Technologies* 58:102214. doi: 10.1016/j.ifset.2019.102214.

Zieliński, H., D. Szawara-Nowak, and M. Wronkowska. 2020. Bioaccessibility of anti-AGEs activity, antioxidant capacity and phenolics from water biscuits prepared from fermented buckwheat flours. *LWT - Food Science and Technology* 123:109051. doi: 10.1016/j.lwt.2020.109051.